5-13-2019 2:00 PM

A pH-sensitive Delivery System for the Prevention of Dental Caries Using Salivary Proteins

Yi Zhu, *The University of Western Ontario*

Supervisor: Gillies, Elizabeth R., *The University of Western Ontario*
Joint Supervisor: Siqueira, Walter L., *The University of Western Ontario*
A thesis submitted in partial fulfillment of the requirements for the Master of Engineering Science degree in Biomedical Engineering

Abstract

Dental caries remains one of the most common chronic diseases worldwide. Salivary proteins such as histatins have demonstrated biological functions directly related to tooth homeostasis and prevention of dental caries. However, histatins are susceptible to the high proteolytic activities in the oral environment. Therefore, pH-sensitive chitosan nanoparticles (CNs) have been proposed as potential carriers to target major oral diseases that occur under acidic conditions (e.g. dental caries and dental erosion). Four different types of chitosan polymers were investigated and the optimized CNs successfully loaded histatin 3 and released it selectively under acidic conditions. Through loading the survival time of histatin 3 was increased by two-fold in diluted whole saliva. Results from biofilm experiment have demonstrated both blank and histatin 3-loaded CNs were able to reduce biofilm growth of *Streptococcus mutans*. The results of this study have demonstrated the potential of using blank CNs alone as antibacterial agent for oral applications in addition to the potential of CNs as protein carriers, especially for diseases occurring at acidic conditions.

Keywords

Chitosan, Nanoparticles, Drug Delivery, Salivary Proteins, Protein Carrier

Co-Authorship Statement

The work presented in this thesis is the result of the author's work as well as the work of coworkers at Western University, and supervisors Dr. Elizabeth Gillies and Dr. Walter Siqueira whose exact contributions are described here.

Chapter 1 was written by the author and edited by Dr. Elizabeth Gillies.

Chapter 2 describes a project proposed by Dr. Elizabeth Gillies and Dr. Walter Siqueira, both of them contributed to the design of the project. Dr. Yizhi Xiao aided in interpreting the results. All of the experiments were carried out by the author. The chapter constitutes a manuscript in preparation, which was written by the author and edited by Dr. Elizabeth Gillies and Dr. Walter Siqueira.

Chapter 3 was written by the author and edited by Dr. Elizabeth Gillies.

Acknowledgments

First of all, I would like to sincerely thank both of my supervisors, Dr. Elizabeth Gillies and Dr. Walter Siqueira for their continuous guidance and endless support throughout my study. It has been a pleasure to be their student.

Secondly, I would like to thank all of my lab mates for the precious memories inside and outside of the lab. Special thanks to Charmaine for proofreading my thesis, and Lina for teaching me all of the microbiology techniques.

Thirdly, I would like to thank my mom for her support, both financially and domestically. Even though I lived away from home for the past two years, she had always prepared one week worth of food whenever I go back home. Words cannot express my gratitude and I'm very grateful.

Lastly, I also want to take this opportunity to thank my girlfriend, Michelle. For showing up fashionably late into my life, otherwise, my thesis couldn't have been this fruitful.

Thank everyone who takes their time to read this thesis!

Table of Contents

List of Tables

List of Figures

List of Abbreviations

AEP	Acquired enamel pellicle
AMPs	Antibacterial peptides
CFU	Colony forming units
CNs	Chitosan nanoparticles
DD	Degree of deacetylation
DLS	Dynamic light scattering
HTNs	Histatins
HTN3	Histatin 3
IC_{50}	Half maximal inhibitory concentration
MW	Molecular weight
OD	Optical density
PAGE	Polyacrylamide gel electrophoresis
PBS	Phosphate buffer faline
PDI	Polydispersity index
S. mutans	*Streptococcus mutans*
TEM	Transmission electron microscopy
THB	Todd hewitt broth
TPP	Sodium tripolyphosphate
TYEB	Tryptone yeast extract broth
WSS	Whole saliva supernatant

Chapter 1

1. Introduction

1.1 Dental Caries and Their Prevalence

Dental caries, also known as tooth decay, remains one of the most common chronic diseases worldwide (Kassebaum et al. 2015; Frencken et al. 2017). Globally, approximately 2.4 billion people (32% of the world population) have experienced dental caries in their permanent teeth (James et al. 2018). The severity of dental caries is dependent on many factors including susceptibility of the tooth surface, the frequency of sugar intake, oral hygiene behavior, and the presence of cariogenic bacteria (Garcia et al. 2017). Untreated dental caries has often been associated with a negative impact on quality of life, such as discomfort caused by toothache, pain-induced lack of appetite, foul breath, prolonged exposure to oral inflammation, and other symptoms.

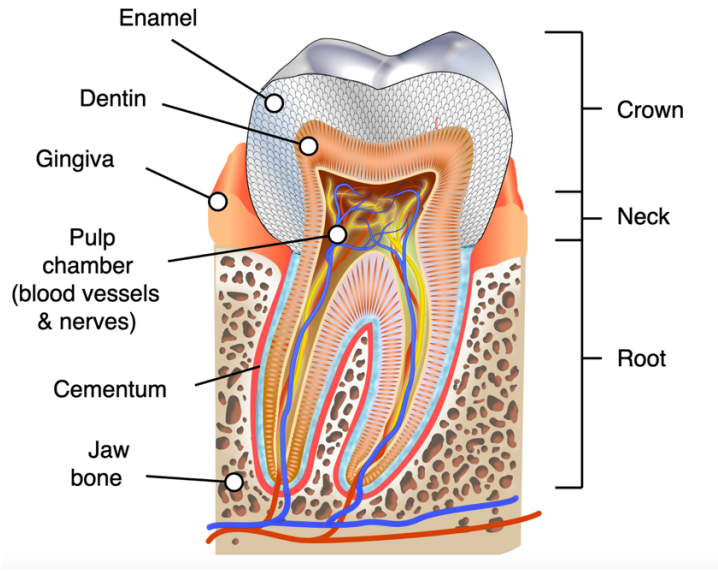

Figure 1.1 Major components of the tooth are displayed. Enamel is the surface layer covering the dentin. Dentin in turn covers the pulp. Extending down to the root, dentin is covered by the cementum. (K.D. Schroeder, human tooth diagram-en.svg from Wikimedia Commons. Licensed under CC BY-SA 4.0.)

The structure of the tooth is presented in Figure 1.1. Enamel is the outermost layer covering the dentin, which covers the pulp. Moving down to the root, the dentin is now covered by the cementum. A caries lesion has penetrated into the dentin from the enamel layer, as labelled on Figure 1.1. There are many stages of dental caries. The carious dissolution of dental hard tissue always starts with the tooth surface. The surface is not limited to enamel surface. Root cementum and exposed dentin are also possible surfaces for caries to develop. However, in most cases, caries usually affects the enamel layer first. At this stage, the damage is still reversible. When the caries reaches into dentin, current treatment requires a filling procedure to be performed. If the caries penetrates deeper into the root of the teeth, this could lead to possible damage of the tooth nerve, which may result in tooth loss and infection (Cochrane et al. 2010; Wong et al. 2017).

Dental caries is a complex multifactorial disease that results in mineral dissolution of the dental hard tissues (enamel, dentin and cementum) by acidic by-products of bacteria through fermentation of dietary carbohydrates. Caries is a dynamic process between pathological and protective factors, as presented in Figure 1.2. Pathological factors include acidogenic bacteria that ferment dietary carbohydrates into different types of acids. These acids then diffuse into the enamel, dentin, or cementum, leading to partial mineral dissolution. Dissolved mineral content (calcium and phosphate) diffuses out of the tooth and the resulting loss in mineral content is known as demineralization (Marsh 2009). This eventually leads to cavitation if the process progresses. Other factors include reduced salivary functions such as reduced saliva flow and imbalanced salivary composition. Increased frequency of carbohydrate intake also increases the risk of caries development. Demineralization can be reversed by the diffusion of minerals like calcium, phosphate, and fluoride. They can be deposited back onto the remaining mineral remnants caused by demineralization (Featherstone 2004). The process of mineral gains is referred to as remineralization (Tung and Eichmiller 2004) and it is promoted by protective factors such as saliva, proteins and fluoride.

The acidic by-products can be neutralized by saliva due to its bicarbonate/carbonate buffering capacity. Fluoride solution or fluoride containing oral products may also promote remineralization (Kanduti et al. 2016). The dynamic process of demineralization and

remineralization happens many times a day, usually after carbohydrate intake from food or drinks. Dental caries occurs when the demineralization process initiated by the pathological factors dominates, and as a result there is a net loss of mineral content. If the balance is shifted towards the remineralization process promoted by protective factors, development of caries stops or reverses.

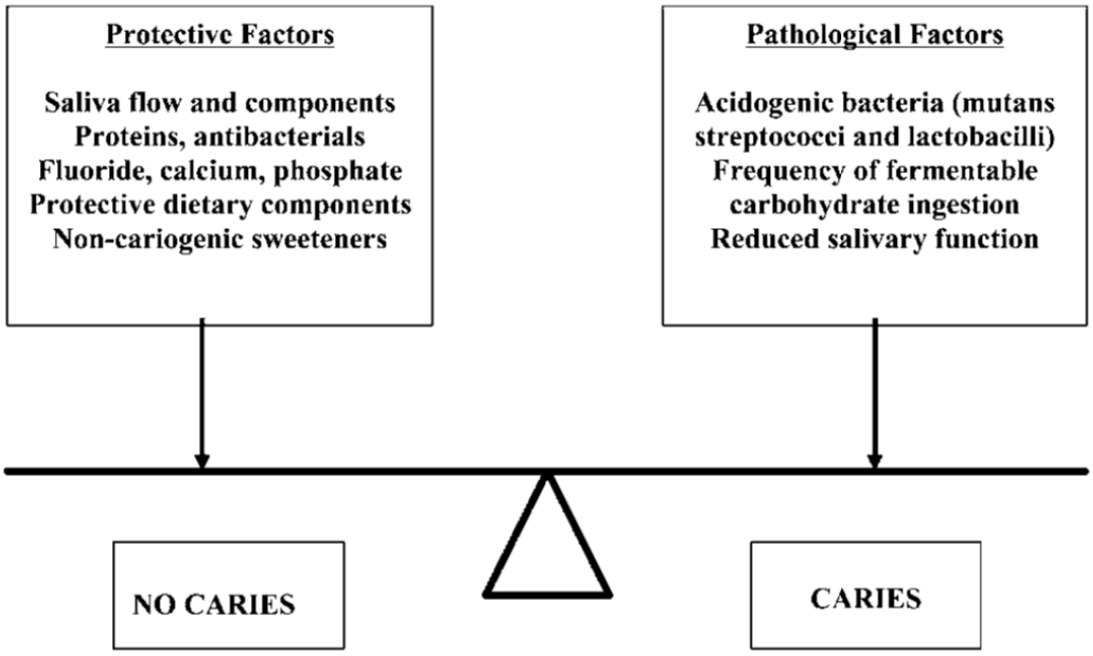

Figure 1.2 Schematic representation of the balance between protective factors and pathological factors and how they affect the development of caries. Reprinted with permission from Featherstone 2004. Copyright 2004 SAGE Publications.

For demineralization to occur, the salivary pH needs to drop below a certain level. The Stephan curve – first described by Stephan and Miller in the 1940s – depicts salivary pH changes in the mouth after rinsing with glucose, corresponding to the pH changes observed in saliva following sugar intake (Bowen 2013). As presented in Figure 1.3, the resting salivary pH without exposure to sugar usually has a pH value between 6 and 7. This varies for each individual, but remains stable until carbohydrate intake (Sissons et al. 1998). The salivary pH was observed to drop rapidly following carbohydrate consumption. The critical level was defined at pH 5.5 where demineralization of the enamel will begin

to occur. The pH level may remain below this critical level for approximately 20 minutes, and recovery to resting pH may take about 30 to 60 mins.

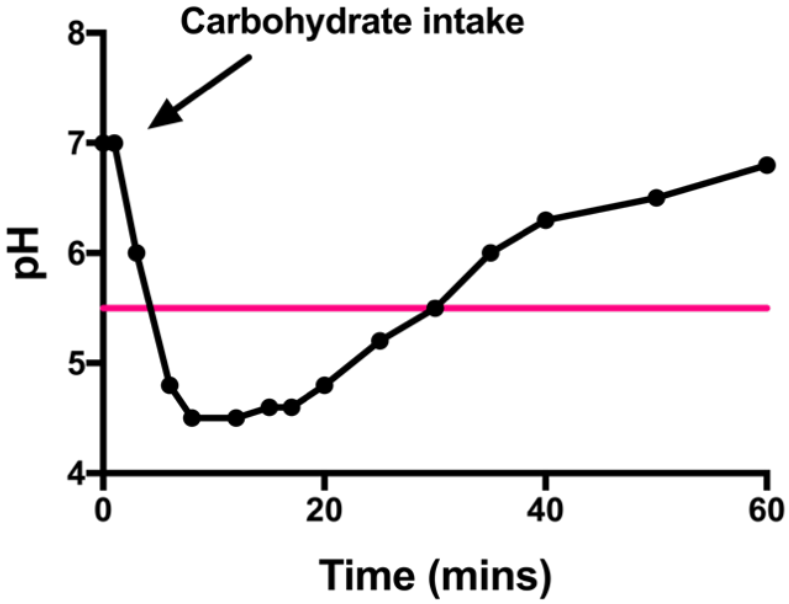

Figure 1.3 Stephan curve illustrating the change in pH following carbohydrate ingestion. The critical level is defined at pH 5.5 and is represented by the pink line. At/below the critical level, demineralization will occur, consequently increasing caries risk.

The most common preventive approach is good oral hygiene practices, including brushing twice a day and the use of dental floss. Regular visits to the dentist for mechanical removal of dental plaque is another effective way to reduce caries risk (Finkelstein et al. 1990). Fluoride treatment is often provided in conjunction with mechanical cleaning, which reduces the demineralization process and promotes remineralization of enamel by absorbing onto the enamel to form fluorohydroxyapatite. The resulting enamel is strengthened and becomes more resistant to demineralization (Buzalaf et al. 2011). Fluoride containing toothpaste is already common in North America and Europe, but it is only effective at concentrations higher than 1,000 ppm. However, the new challenge that arises is the increased frequency of daily sugar consumption. As illustrated in Figure 1.4,

frequent snack/coffee breaks between meals result in increased exposure to cariogenic (acidic) environments. The extended duration of exposure to pH under the critical level (pH 5.5) can promote demineralization, which increases the risk of caries development. A potential effective preventive approach would be to inhibit bacterial activity to prevent or shorten the demineralization process.

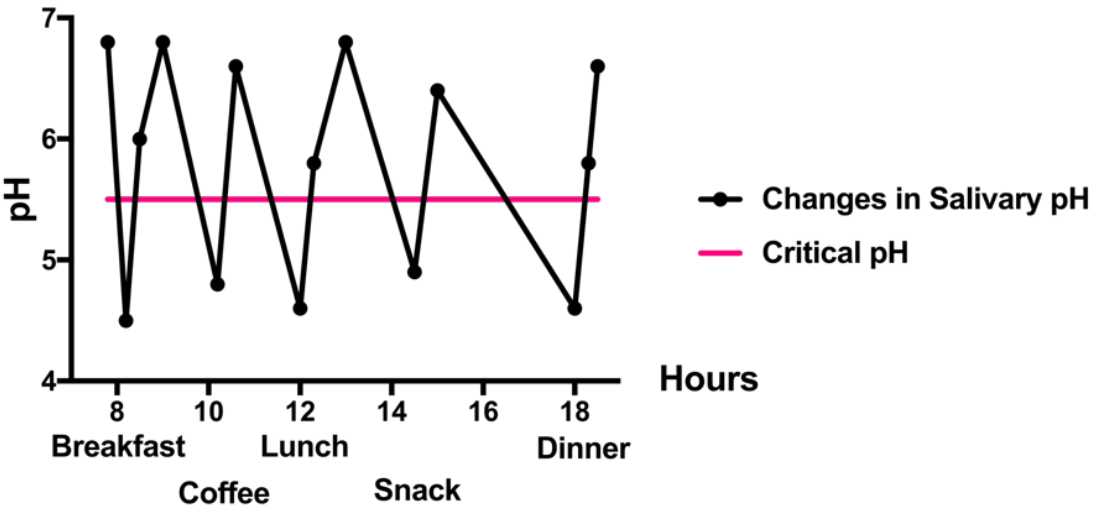

Figure 1.4 Frequent sugar intake increases exposure to acidic conditions, which can increase caries risk.

1.2 AEP and its Role in Regulating Biofilm Formation

Saliva is another protective factor that was mentioned in the previous section. It is a complex fluid composed of proteins, enzymes, and a variety of electrolytes. Many physiological functions are regulated by saliva, such as chewing, initial digestion of food, wetting, and lubrication (Humphrey and Williamson 2001; Siqueira and Dawes 2011). Saliva also plays an active role in the maintenance of oral health, including partial protection against microbial activities, the maintenance of both salivary pH and tooth integrity (Mandel 1987). The inorganic ions present in saliva are mainly calcium and phosphate. They remain at a supersaturation state with respect to hydroxyapatite (HA)

crystal, the major component of tooth enamel. This supersaturation of calcium and phosphate ions promotes remineralization of the tooth enamel by allowing the diffusion of these ions into the HA. However, the remineralization process is mainly regulated by salivary proteins which constitute the acquired enamel pellicle (AEP) (Valente et al. 2018).

AEP is a thin proteinaceous film formed on the tooth surface by selective adsorption of salivary proteins and other molecules present in the oral fluids. Its formation is initiated within seconds of exposure to whole saliva after oral cleaning (Siqueira et al. 2012). AEP serves as a platform which allows bacterial adhesion for the development of biofilm. The oral cavity harbors many different types of microorganisms. Some of the primary colonizers which attach themselves to the AEP are the *Streptococcus species*, *Actinomyces species* and *Haemophilus species* (Dige et al. 2009; Huang et al. 2011; Dorkhan et al. 2013). Secondary colonizers such as *Fusobacterium nucleatum*, *Treponema species*, and *Tannerella forsythensis*, bind onto already attached primary bacteria by co-adhesion or co-aggregation (Kolenbrander et al. 2002; Foster and Kolenbrander 2004). The composition of the biofilm becomes more diversified. The mature biofilm is commonly known as a dental plaque. The dental plaque remains relatively stable over time under microbial homeostasis. However, when the microbial composition favors acidogenic species such as *Streptococcus mutans* (*S. mutans*) (Marsh 2006), the extended exposure to acidic conditions initiates demineralization and paves the way for the development of caries.

AEP serves multiple functions due to its physical structure and salivary proteins. The physical structure prevents direct contact between acids produced by acidogenic bacteria and the tooth surface. This intervention reduces mineral dissolution of the tooth (Moreno and Zahradnik 1979; Hannig et al. 2004; Hara et al. 2006). The physical structure also plays a crucial role in regulating the attachment of early microbial colonizers. Therefore, it is reasonable to propose that modulation of the composition or structure of the AEP is a potential preventive approach for dental caries. In previous research, salivary proteins identified from the AEP such as histatin (HTN) and statherin have demonstrated strong affinity for HA. The ability of the proteins to prevent the precipitation of calcium and phosphate on tooth enamel (Valente et al. 2018) in addition to modulation of the AEP structure could also potentially affect attachment of cariogenic bacteria.

1.3 Discovery of Salivary Proteins and Their Functions

Salivary proteins play a crucial role in regulating oral homeostasis, either by directly exerting antimicrobial effects or interference with microbial colonization. Examples of these antimicrobial peptides (AMPs) include cathelicidin peptide LL-37, alpha-defensins, beta-defensins, HTN and statherin. Other salivary proteins that are present include major glycoproteins (mucins, proline-rich proteins and immunoglobulins) and minor glycoproteins (agglutinin, lactoferrin, cystatins and lysozyme) (Hemadi et al. 2017).

In particular, AMPs have received attention due to their innate immunity. They are often thought of as the first line of defense against oral infection (Brogden 2005). The HTN family is of great interest because these proteins are multifunctional. They have demonstrated biological functions including the inhibition of calcium and phosphate precipitation on enamel, and antimicrobial activities which are directly related to the regulation of oral homeostasis (Oppenheim et al. 2007; Siqueira et al. 2010; Walter L. Siqueira et al. 2012). HTN family proteins are characterized by histidine-rich structures ranging from 7 to 38 amino acids (Johnson et al. 2000). The most commonly expressed forms are HTN1, HTN3, and HTN5, which have molecular weights of 4929, 4063, and 3037 Daltons respectively. Each form comprises about 20-30% of the total HTN pool (Gusman et al. 2004). HTN1 is postulated to play a role in reducing bacterial binding because it is one of the salivary proteins that constitutes the AEP. Previous studies have demonstrated its potential in reducing *S. mutans* adhesion onto HA discs by inhibiting the adsorption of *S. mutans*-binding salivary glycoproteins (Shimotoyodome et al. 2006; Vitorino et al. 2008). HTN5 has the most potent antifungal activity against *Candida albicans*, which is a pathogenic yeast (Puri and Edgerton 2014) that can survive under highly acidic environments and has a high affinity for HA substrates. It also can promote demineralization by dissolving HA through loss of calcium ions (Klinke et al. 2009). HTN3 was demonstrated to be the most effective in killing *S. mutans* (Basiri et al. 2017), which is the most common cariogenic bacterial species present in dental plaque. Through metabolization of dietary sucrose *S. mutans* can produce sticky polysaccharides which function as platforms for further bacterial attachment on the tooth surface. Other simple

sugars can also be digested to produce acidic products. The acidic environment causes the mineral-rich tooth enamel to become susceptible to mineral dissolution. HTN3 has the potential to inhibit bacterial activities, possibly preventing or shortening the demineralization process, and therefore decreasing caries risk.

Statherin is another salivary protein derived from the AEP, and has been observed to have a strong binding affinity and fast adsorption to HA (Zimmerman et al. 2013). Previous studies have demonstrated its ability to regulate calcium phosphate homeostasis. The presence of a covalently linked phosphate group at residues 2 and 3 in statherin peptides can modulate the effect of crystal growth inhibition on HA. This ability makes it a significant contributor to the maintenance of the supersaturation states of calcium and phosphate in saliva (Xiao et al. 2015). Supersaturation of calcium and phosphate is important because it allows enamel to remineralize after transient mineral loss, and inhibits the formation of dental calculus (Hay et al. 1984). Notably, due to proteolytic degradation, statherin levels are substantially lower in whole saliva than in salivary gland secretion (Oppenheim et al. 2007). Therefore, this prevents statherin from being used directly for protein-mediated homeostasis therapeutic.

1.4 Polymer-based Delivery Systems

Despite the multifunctionality of salivary proteins, they are often present in low concentrations (Fábián et al. 2012) due to their susceptibility to the high proteolytic activity in the oral environment (Helmerhorst et al. 2006). Therefore, to use these proteins as potential therapeutics, a delivery system is needed to encapsulate them thereby affording protection against enzymatic degradation.

The utilization of stimulus-responsive polymeric nanoparticles to deliver therapeutics has gained substantial attention in the past decade. Smart delivery systems offer many advantages over conventional dosage forms. Polymeric delivery systems have the potential to improve overall stability, prolong circulation time, and modulate pharmacokinetics, often with reduced toxicity and enhanced efficacy (Mihu et al. 2010;

Yang et al. 2010; Shen et al. 2012; Xiong et al. 2012). Ideally, therapeutics of interest would remain stable inside the delivery system in the absence of a stimulus. Upon stimulus exposure, the delivery system will trigger the release of encapsulated therapeutics. As illustrated in Figure 1.5, stimuli are often categorized based on their properties. Biological cues include enzymes and receptors. Chemical stimuli consist of pH, ionic strength, and electrochemical signals. Lastly, physical stimuli include light, temperature, magnetic field, and ultrasound. Different stimuli-responsive systems can be designed to selectively respond to transient environmental changes that reflect the pathogenic state (Lee et al. 2003; Basel et al. 2011; Chen et al. 2014).

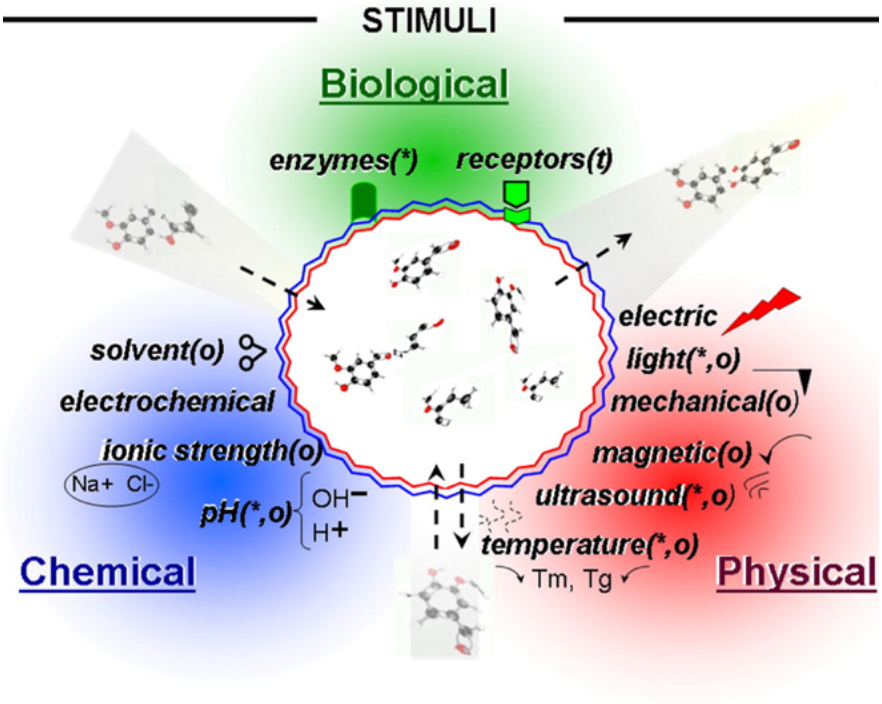

Figure 1.5 Stimuli utilized in drug delivery applications are categorized based on their properties. For example, physical stimuli include temperature, light and ultrasound. Reprinted with permission from Delcea et al. 2011. Copyright 2011 Elsevier.

Many polymeric materials have been explored to prepare a nanoparticle-based delivery system. Two main categories are natural and synthetic polymers (Blasi et al. 2007; Kumari et al. 2010). In particular, naturally occurring polymers are of great interest because of their unique physical and biological properties. This category includes polysaccharides,

proteins, and polyisoprenes (Ravve 2000). Polysaccharides are polymers of monosaccharides that are abundant in nature. They have a variety of functional groups, which contribute to their diversified structures and properties. In recent years, research has demonstrated the suitability of polysaccharides, including alginate, chitosan and starch as potential candidates for applications in a nanoparticle-based drug delivery system (Anirudhan et al. 2017; Choudhary et al. 2019; Zheng et al. 2019).

As the only naturally occurring polycationic polysaccharide discovered so far and with its ability to interact with anionic molecules, chitosan and its derivatives have been studied extensively for applications in the agricultural, medicinal and pharmaceutical industries (Souza et al. 2014; Bugnicourt and Ladavière 2016; Olivera et al. 2016). Chitosan is a copolymer composed of *N*-acetyl-D-glucosamine and β (1-4) linked D-glucosamine. It is prepared by treating natural polymer chitin with alkaline chemicals, through a process called deacetylation. Chitin is a primary structural component found in the cell walls of fungi, exoskeletons of crustaceans, and is one of the most abundant polysaccharides existing in nature (Ravi Kumar 2000). Chitosan also offers other advantages including biodegradability (Kean and Thanou 2010), biocompatibility (Thandapani et al. 2017), and pH-dependent solubility (Cha et al. 2006). As demonstrated in Figure 1.6, under high pH conditions, the amino group becomes deprotonated, resulting in a low solubility in water. Consequently, the polymer chains will cluster together to form a more compact structure. When the amino group is protonated under low pH conditions, the increased solubility in water allows the polymer chain to exhibit a more extended structure.

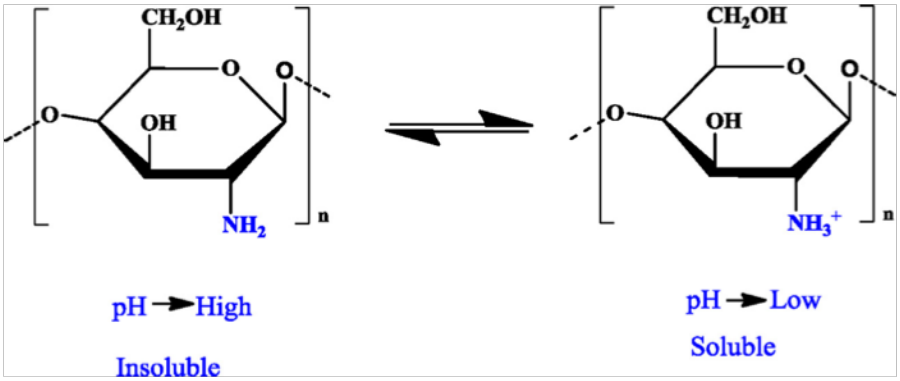

Figure 1.6 Structural changes of chitosan affect its solubility. When the amino group is protonated under low pH conditions, it becomes more soluble. Solubility is low when the amino group becomes deprotonated under high pH conditions. Reprinted with permission from Ali and Ahmed 2018. Copyright 2018 Elsevier.

Chitosan-based delivery systems have been explored due to their aforementioned advantageous properties. Chitosan has been formulated into different carriers such as microspheres (Zhang et al. 2013), hydrogels (Sadat Ebrahimi and Schönherr 2014), beads (Chandy and Sharma 1992) and nanoparticles (Sarmento et al. 2007). For the delivery of small proteins/peptides, nanoparticles are more advantageous because of their high surface area to volume ratios. There are many different methods to synthesize chitosan nanoparticles (CNs). Some common approaches are ionic gelation, covalent cross-linking, emulsification solvent diffusion and self-assembly.

Ionic gelation occurs through electrostatic interactions between chitosan or its derivatives with an ionic cross-linking agent of opposite charge. Among polyanionic cross-linking agents, the most commonly used is sodium tripolyphosphate (TPP), which is non-toxic and widely used as a preservative in the food industry (Kawashima et al. 1985). In this method, chitosan polymer is dissolved in acetic acid, while TPP is dissolved in Millipore water. The TPP solution is then added into the chitosan solution in a drop-wise manner under constant mechanical stirring. Positively charged chitosan polymer chains interact electrostatically with the negatively charged TPP under mechanical stirring, as illustrated in Figure 1.7. The advantages of this method include its simplicity to perform and scale up, as it can be performed at room temperature without the use of any organic

solvent. Previous studies have investigated the ability of CNs prepared via ionic gelation to encapsulate peptides/proteins, oligonucleotides, and drugs for potential pharmaceutical applications (Sezer and Akbuğa 1995; Aydin and Akbuğa 1996; Shu and Zhu 2000).

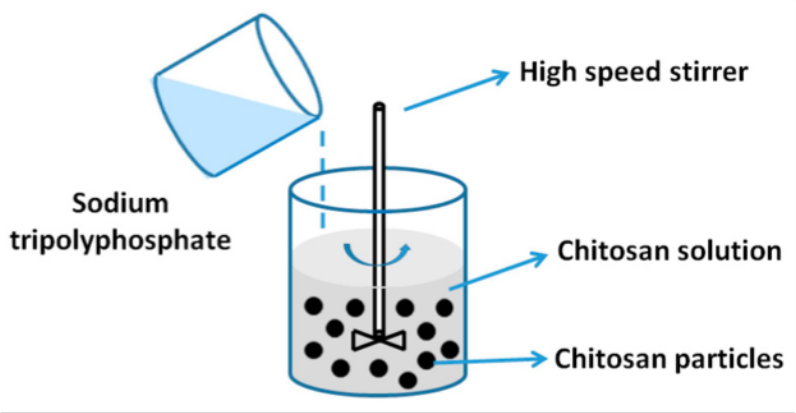

Figure 1.7 CNs prepared by ionic gelation with TPP, TPP solution was added to chitosan solution in a drop-wise manner under constant mechanical stirring, CNs will form based on the electrostatic interactions between the two oppositely charge species. Reprinted from Wang et al. 2016. Licensed under CC BY 4.0.

Another technique for preparing CNs is through covalent cross-linking (Prabaharan and Mano 2005). This involves the formation of a covalent bond between the chitosan polymer chain with a cross-linking agent. Some functional groups that could be covalently attached to the amino groups on the chitosan chain include polyethylene glycol, dicarboxylic acid, and glutaraldehyde (Bodnar et al. 2005; Goldberg et al. 2007). This method was first used to prepare chitosan nanoparticles by cross-linking with glutaraldehyde to encapsulate 5-fluorouracil (Ohya et al. 1993).

CNs can also be prepared by emulsification solvent diffusion method. An emulsion is prepared by injecting an organic solvent into chitosan solution under high-pressure homogenization. Subsequently, a large amount of water is added to the emulsion. Polymer precipitation occurs following the diffusion of organic solvent into water, consequently leading to the formation of CNs (El-Shabouri 2002). This method is desirable to

encapsulate hydrophobic drugs with a high encapsulation efficiency. However, the major disadvantages are the use of organic solvent and high shear forces (Wang et al. 2016).

Self-assembly of nanoparticles refers to the process of spontaneous formation of nanoparticles when amphiphilic compounds are dispersed in water. A core-shell structure will be formed with a hydrophilic moiety on the periphery and a hydrophobic moiety clustered in the core. The main advantage of this method is that poorly water-soluble molecules, such as anticancer drugs, can be successfully loaded into the hydrophobic core of modified CNs. One previous study used chemically modified glycol chitosan with hydrophobic cholinic acid and prepared nanoparticles via self-assembly after dispersion in water solution. The hydrophobic core successfully encapsulated the poorly water-soluble anticancer drug cisplatin with a drug loading of 80%. Through encapsulation, cisplatin was released in a sustained manner for a week, and the toxicity profile was also improved (Kim et al. 2008). Another study involved modified chitosan polymer with alkyl chains as the hydrophobic moiety and glycol groups as the hydrophilic moiety. The synthesized CNs were able to improve the solubility of the poorly water-soluble antitumor drug paclitaxel by 500-fold, at a drug loading of 35% (Huo et al. 2010).

CNs can encapsulate a variety of cargo aside from anticancer drugs, which include gene therapeutics, protein drugs, and more (Sarmento et al. 2007; Han et al. 2010). CNs can be administered orally, nasally, and intravenously. Most cargo cannot survive for very long when administered on their own. For example, gene silencing mediated by siRNA has demonstrated potential for treating diseases caused by genetic defects. However, when delivered alone, it faces challenges including rapid degradation and poor cellular uptake. Through encapsulation of CNs prepared via ionic gelation between chitosan and TPP, CNs were able to protect siRNA against degradation by nucleases. The positive charge of siRNA CNs also improved adsorption onto the cell surface. However, gene transfection efficiency was low as a result of encapsulation (Katas and Alpar 2006). This was later addressed by optimizing the properties of chitosan, including molecular weight and degree of deacetylation. With chemical modification of chitosan using folic acid, the optimized folic acid modified CNs were able to demonstrate an equivalent transfection efficiency compared against the positive control group (Lavertu et al. 2006) .

Protein drugs are susceptible to enzymatic degradation and therefore have poor overall stability and short survival time. In the past, insulin and a cationic β-cyclodextrin complex has been encapsulated into alginate-CNs. The delivery system was not only able to protect insulin against degradation from simulated gastric fluid, but it also cumulatively released approximately 40% of the encapsulated insulin under simulated intestinal fluid (Zhang et al. 2010).

1.5 Rationale and Focus of this Work

In the current work, HTN3 has been selected as the protein of interest due to its antibacterial property against *S. mutans*. Through loading of HTN3 within CNs, the delivery system should remain stable at physiological salivary pH to protect the loaded HTN3 against enzymatic degradation. The pH-responsive property of CNs should allow selective release of HTN3 under acidic conditions, as shown below in Figure 1.8.

The pH-responsive behaviour of HTN3-loaded CNs is important, because the salivary pH drops every time after carbohydrate intake. The acidic conditions promote major oral complications such as dental caries and dental erosion (Nikaido et al. 2004). The drop in pH should trigger the immediate release of loaded HTN3. The released HTN3 may inhibit bacterial fermentation of ingested carbohydrate, possibly preventing or shortening the exposure to acidic environment and reducing demineralization.

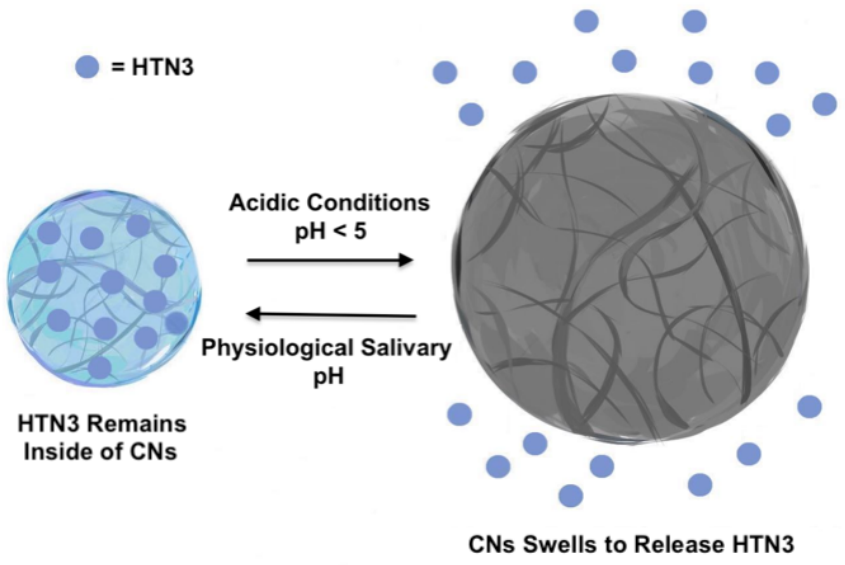

Figure 1.8 A schematic representation of the pH-sensitive release mechanism exhibited by CNs. HTN3 remains inside of CNs under physiological salivary pH. The CNs will swell selectively under acidic conditions to release loaded HTN3.

1.6 Thesis Outline

The central hypothesis of this thesis is that I can develop a pH-sensitive CN delivery system, which can be utilized to load multifunctional salivary proteins for targeting major oral complications that occur under acidic conditions.

Chapter 2, describes the study of different types of chitosan polymers to select the optimal CNs formulation. The optimized CNs formulation was characterized by dynamic light scattering and visualized by transmission electron microscopy. The pH-responsive property of the CNs was also assessed through pH-dependent swelling and pH cycling studies. Secondly, the protein of interest, HTN3 was loaded into CNs and different protein loading ratios were studied thoroughly. Cumulative and pH cycling release profiles under different pH conditions were also evaluated. Additionally, a protein degradation study was performed to evaluate the protection offered by loading against enzymatic degradation. Lastly, the therapeutic effect of HTN3-loaded CNs against *S. mutans* biofilm formation on

hydroxyapatite discs was evaluated based on biofilm weight and bacterial cell viability. The results were compared against four other treatment groups: PBS (control), free HTN3, unloaded CNs, and gold standard fluoride solution.

In chapter 3, a general conclusion is presented based on the collected data. The significance, possible improvements, and future work regarding this project are also discussed.

The ultimate goal of this project is to formulate CN-based dental hygiene products like toothpaste and mouthwash. With the development of HTN3-loaded CNs, the results of this work could potentially advance the delivery of salivary proteins as a preventive measure to address dental caries.

1.7 References

Ali A, Ahmed S. 2018. A review on chitosan and its nanocomposites in drug delivery. Int J Biol Macromol. 109(Complete):273–286. doi:10.1016/j.ijbiomac.2017.12.078.

Anirudhan TS, Anila MM, Franklin S. 2017. Synthesis characterization and biological evaluation of alginate nanoparticle for the targeted delivery of curcumin. Mater Sci Eng C. 78(Complete):1125–1134. doi:10.1016/j.msec.2017.04.116.

Aydin Z, Akbuğa J. 1996. Chitosan beads for the delivery of salmon calcitonin: Preparation and release characteristics. Int J Pharm. 131(1):101–103. doi:10.1016/0378-5173(95)04300-4.

Basel MT, Shrestha TB, Troyer DL, Bossmann SH. 2011. Protease-Sensitive, Polymer-Caged Liposomes: A Method for Making Highly Targeted Liposomes Using Triggered Release. ACS Nano. 5(3):2162–2175. doi:10.1021/nn103362n.

Basiri T, Johnson ND, Moffa EB, Mulyar Y, Serra Nunes PL, Machado M a. a. M, Siqueira WL. 2017. Duplicated or Hybridized Peptide Functional Domains Promote Oral Homeostasis. J Dent Res. 96(10):1162–1167. doi:10.1177/0022034517708552.

Blasi P, Giovagnoli S, Schoubben A, Ricci M, Rossi C. 2007. Solid lipid nanoparticles for targeted brain drug delivery. Adv Drug Deliv Rev. 59(6):454–477. doi:10.1016/j.addr.2007.04.011.

Bodnar M, Hartmann JF, Borbely J. 2005. Preparation and characterization of chitosan-based nanoparticles. Biomacromolecules. 6(5):2521–2527. doi:10.1021/bm0502258.

Bowen W. 2013. The Stephan Curve revisited. Odontology. 101(1):2–8. doi:10.1007/s10266-012-0092-z.

Brogden KA. 2005. Antimicrobial peptides: pore formers or metabolic inhibitors in bacteria? Nat Rev Microbiol. 3(3):238-.

Bugnicourt L, Ladavière C. 2016. Interests of chitosan nanoparticles ionically cross-linked with tripolyphosphate for biomedical applications. Prog Polym Sci. 60(Complete):1–17. doi:10.1016/j.progpolymsci.2016.06.002.

Buzalaf MAR, Pessan JP, Honório HM, ten Cate JM. 2011. Mechanisms of action of fluoride for caries control. Monogr Oral Sci. 22:97–114. doi:10.1159/000325151.

Cha J, Lee WB, Park CR, Cho YW, Ahn C-H, Kwon IC. 2006. Preparation and characterization of cisplatin-incorporated chitosan hydrogels, microparticles, and nanoparticles. Macromol Res. 14(5):573–578. doi:10.1007/BF03218726.

Chandy T, Sharma CP. 1992. Chitosan beads and granules for oral sustained delivery of nifedipine: in vitro studies. Biomaterials. 13(13):949–952.

Chen K-J, Chaung E-Y, Wey S-P, Lin K-J, Cheng F, Lin C-C, Liu H-L, Tseng H-W, Liu C-P, Wei M-C, et al. 2014. Hyperthermia-Mediated Local Drug Delivery by a Bubble-Generating Liposomal System for Tumor-Specific Chemotherapy. ACS Nano. 8(5):5105–5115. doi:10.1021/nn501162x.

Choudhary RC, Kumaraswamy RV, Kumari S, Sharma SS, Pal A, Raliya R, Biswas P, Saharan V. 2019. Zinc encapsulated chitosan nanoparticle to promote maize crop yield. Int J Biol Macromol. 127:126–135. doi:10.1016/j.ijbiomac.2018.12.274.

Cochrane NJ, Cai F, Huq NL, Burrow MF, Reynolds EC. 2010. New Approaches to Enhanced Remineralization of Tooth Enamel. J Dent Res. 89(11):1187–1197. doi:10.1177/0022034510376046.

Delcea M, Möhwald H, Skirtach AG. 2011. Stimuli-responsive LbL capsules and nanoshells for drug delivery. Adv Drug Deliv Rev. 63(9):730–747. doi:10.1016/j.addr.2011.03.010.

Dige I, Raarup MK, Nyengaard JR, Kilian M, Nyvad B. 2009. Actinomyces naeslundii in initial dental biofilm formation. Microbiology. 155(7):2116–2126. doi:10.1099/mic.0.027706-0.

Dorkhan M, Svensäter G, Davies JR. 2013. Salivary pellicles on titanium and their effect on metabolic activity in Streptococcus oralis. BMC Oral Health. 13(1):32. doi:10.1186/1472-6831-13-32.

El-Shabouri MH. 2002. Positively charged nanoparticles for improving the oral bioavailability of cyclosporin-A. Int J Pharm. 249(1–2):101–108.

Fábián TK, Hermann P, Beck A, Fejérdy P, Fábián G. 2012. Salivary defense proteins: their network and role in innate and acquired oral immunity. Int J Mol Sci. 13(4):4295–4320. doi:10.3390/ijms13044295.

Featherstone JDB. 2004. The Continuum of Dental Caries—Evidence for a Dynamic Disease Process. 83(1_suppl):39–42.

Finkelstein P, Yost KG, Grossman E. 1990. Mechanical devices versus antimicrobial rinses in plaque and gingivitis reduction. Clin Prev Dent. 12(3):8–11.

Foster JS, Kolenbrander PE. 2004. Development of a multispecies oral bacterial community in a saliva-conditioned flow cell. Appl Environ Microbiol. 70(7):4340–4348. doi:10.1128/AEM.70.7.4340-4348.2004.

Frencken JE, Sharma P, Stenhouse L, Green D, Laverty D, Dietrich T. 2017. Global epidemiology of dental caries and severe periodontitis – a comprehensive review. J Clin Periodontol. 44:S94–S105. doi:10.1111/jcpe.12677.

Garcia SS, Blackledge MS, Michalek S, Su L, Ptacek T, Eipers P, Morrow C, Lefkowitz EJ, Melander C, Wu H. 2017. Targeting of Streptococcus mutans Biofilms by a Novel Small Molecule Prevents Dental Caries and Preserves the Oral Microbiome. J Dent Res. 96(7):807–814. doi:10.1177/0022034517698096.

Goldberg M, Langer R, Jia X. 2007. Nanostructured materials for applications in drug delivery and tissue engineering. J Biomater Sci Polym Ed. 18(3):241–268.

Gusman H, Leone C, Helmerhorst EJ, Nunn M, Flora B, Troxler RF, Oppenheim FG. 2004. Human salivary gland-specific daily variations in histatin concentrations determined by a novel quantitation technique. Arch Oral Biol. 49(1):11–22. doi:10.1016/S0003-9969(03)00182-1.

Han HD, Mangala LS, Lee JW, Shahzad MMK, Kim HS, Shen D, Nam EJ, Mora EM, Stone RL, Lu C, et al. 2010. Targeted Gene Silencing Using RGD-Labeled Chitosan Nanoparticles. Clin Cancer Res. 16(15):3910–3922. doi:10.1158/1078-0432.CCR-10-0005.

Hannig M, Fiebiger M, Güntzer M, Döbert A, Zimehl R, Nekrashevych Y. 2004. Protective effect of the in situ formed short-term salivary pellicle. Arch Oral Biol. 49(11):903–910. doi:10.1016/j.archoralbio.2004.05.008.

Hara AT, Ando M, González-Cabezas C, Cury JA, Serra MC, Zero DT. 2006. Protective Effect of the Dental Pellicle against Erosive Challenges in situ. J Dent Res. 85(7):612–616. doi:10.1177/154405910608500706.

Hay DI, Smith DJ, Schluckebier SK, Moreno EC. 1984. Relationship between concentration of human salivary statherin and inhibition of calcium phosphate precipitation in stimulated human parotid saliva. J Dent Res. 63(6):857–863. doi:10.1177/00220345840630060901.

Helmerhorst EJ, Alagl AS, Siqueira WL, Oppenheim FG. 2006. Oral fluid proteolytic effects on histatin 5 structure and function. Arch Oral Biol. 51(12):1061–1070. doi:10.1016/j.archoralbio.2006.06.005.

Hemadi AS, Huang R, Zhou Y, Zou J. 2017. Salivary proteins and microbiota as biomarkers for early childhood caries risk assessment. Int J Oral Sci. 9(11):e1. doi:10.1038/ijos.2017.35.

Huang R, Li M, Gregory RL. 2011. Bacterial interactions in dental biofilm. Virulence. 2(5):435. doi:10.4161/viru.2.5.16140.

Humphrey SP, Williamson RT. 2001. A review of saliva: Normal composition, flow, and function. J Prosthet Dent. 85(2):162–169. doi:10.1067/mpr.2001.113778.

Huo M, Zhang Y, Zhou J, Zou A, Yu D, Wu Y, Li J, Li H. 2010. Synthesis and characterization of low-toxic amphiphilic chitosan derivatives and their application as

micelle carrier for antitumor drug. Int J Pharm. 394(1):162–173. doi:10.1016/j.ijpharm.2010.05.001.

James SL, Abate D, Abate KH, Abay SM, Abbafati C, Abbasi N, Abbastabar H, Abd-Allah F, Abdela J, Abdelalim A, et al. 2018. Global, regional, and national incidence, prevalence, and years lived with disability for 354 diseases and injuries for 195 countries and territories, 1990–2017: a systematic analysis for the Global Burden of Disease Study 2017. The Lancet. 392(10159):1789–1858. doi:10.1016/S0140-6736(18)32279-7.

Johnson DA, Yeh C-K, Dodds MWJ. 2000. Effect of donor age on the concentrations of histatins in human parotid and submandibular/sublingual saliva. Arch Oral Biol. 45(9):731–740. doi:10.1016/S0003-9969(00)00047-9.

Kanduti D, Sterbenk P, Artnik B. 2016. FLUORIDE: A REVIEW OF USE AND EFFECTS ON HEALTH. Mater Socio-Medica. 28(2):133–137. doi:10.5455/msm.2016.28.133-137.

Kassebaum NJ, Bernabé E, Dahiya M, Bhandari B, Murray CJL, Marcenes W. 2015. Global Burden of Untreated Caries: A Systematic Review and Metaregression. J Dent Res. 94(5):650–658. doi:10.1177/0022034515573272.

Katas H, Alpar HO. 2006. Development and characterisation of chitosan nanoparticles for siRNA delivery. J Control Release Off J Control Release Soc. 115(2):216–225. doi:10.1016/j.jconrel.2006.07.021.

Kawashima Y, Handa T, Kasai A, Takenaka H, Lin SY, Ando Y. 1985. Novel method for the preparation of controlled-release theophylline granules coated with a polyelectrolyte complex of sodium polyphosphate-chitosan. J Pharm Sci. 74(3):264–268.

Kean T, Thanou M. 2010. Biodegradation, biodistribution and toxicity of chitosan. Adv Drug Deliv Rev. 62(1):3–11. doi:10.1016/j.addr.2009.09.004.

Kim J-H, Kim Y-S, Park K, Lee S, Nam HY, Min KH, Jo HG, Park JH, Choi K, Jeong SY, et al. 2008. Antitumor efficacy of cisplatin-loaded glycol chitosan nanoparticles in tumor-bearing mice. J Control Release Off J Control Release Soc. 127(1):41–49. doi:10.1016/j.jconrel.2007.12.014.

Klinke T, Kneist S, De Soet JJ, Kuhlisch E, Mauersberger S, Förster A, Klimm W. 2009. Acid Production by Oral Strains of Candida albicans and Lactobacilli. Caries Res Basel. 43(2):83–91.

Kolenbrander PE, Andersen RN, Blehert DS, Egland PG, Foster JS, Palmer RJ. 2002. Communication among Oral Bacteria. Microbiol Mol Biol Rev. 66(3):486–505. doi:10.1128/MMBR.66.3.486-505.2002.

Kumari A, Yadav SK, Yadav SC. 2010. Biodegradable polymeric nanoparticles based drug delivery systems. Colloids Surf B Biointerfaces. 75(1):1–18. doi:10.1016/j.colsurfb.2009.09.001.

Lavertu M, Méthot S, Tran-Khanh N, Buschmann MD. 2006. High efficiency gene transfer using chitosan/DNA nanoparticles with specific combinations of molecular weight and degree of deacetylation. Biomaterials. 27(27):4815–4824. doi:10.1016/j.biomaterials.2006.04.029.

Lee ES, Shin HJ, Na K, Bae YH. 2003. Poly(l-histidine)–PEG block copolymer micelles and pH-induced destabilization. J Controlled Release. 90(3):363–374. doi:10.1016/S0168-3659(03)00205-0.

Mandel ID. 1987. The Functions of Saliva. J Dent Res. 66(2_suppl):623–627. doi:10.1177/00220345870660S203.

Marsh PD. 2006. Dental plaque as a biofilm and a microbial community – implications for health and disease. BMC Oral Health. 6(Suppl 1):S14. doi:10.1186/1472-6831-6-S1-S14.

Marsh PD. 2009. Dental plaque as a biofilm: the significance of pH in health and caries. Compend Contin Educ Dent Jamesburg NJ 1995. 30(2):76–78, 80, 83–87; quiz 88, 90.

Meyer-Lueckel H, Paris S, Ekstrand KR. 2013. Caries management: science and clinical practice. New York (NY): Stuttgart Thieme. 409 p.

Mihu MR, Sandkovsky U, Han G, Friedman JM, Nosanchuk JD, Martinez LR. 2010. The use of nitric oxide releasing nanoparticles as a treatment against Acinetobacter baumannii in wound infections. Virulence. 1(2):62–67. doi:10.4161/viru.1.2.10038.

Moreno EC, Zahradnik RT. 1979. Demineralization and Remineralization of Dental Enamel. J Dent Res. 58(2):896–903. doi:10.1177/00220345790580024301.

Nikaido T, Moriya K, Hiraishi N, Ikeda M, Kitasako Y, Foxton RM, Tagami J. 2004. Surface analysis of dentinal caries in primary teeth using a pH-imaging microscope. Dent Mater J. 23(4):628–632.

Ohya Y, Takei T, Kobayashi H, Ouchi T. 1993. Release behaviour of 5-fluorouracil from chitosan-gel microspheres immobilizing 5-fluorouracil derivative coated with polysaccharides and their cell specific recognition. J Microencapsul. 10(1):1–9. doi:10.3109/02652049309015307.

Olivera S, Muralidhara HB, Venkatesh K, Guna VK, Gopalakrishna K, Kumar K. Y. 2016. Potential applications of cellulose and chitosan nanoparticles/composites in wastewater treatment: A review. Carbohydr Polym. 153(Complete):600–618. doi:10.1016/j.carbpol.2016.08.017.

Oppenheim FG, Salih E, Siqueira WL, Zhang W, Helmerhorst EJ. 2007. Salivary proteome and its genetic polymorphisms. Ann N Y Acad Sci. 1098:22–50. doi:10.1196/annals.1384.030.

Prabaharan M, Mano JF. 2005. Chitosan-based particles as controlled drug delivery systems. Drug Deliv. 12(1):41–57.

Puri S, Edgerton M. 2014. How Does It Kill?: Understanding the Candidacidal Mechanism of Salivary Histatin 5. Eukaryot Cell. 13(8):958–964. doi:10.1128/EC.00095-14.

Ravi Kumar MNV. 2000. A review of chitin and chitosan applications. React Funct Polym. 46(1):1–27. doi:10.1016/S1381-5148(00)00038-9.

Ravve A. 2000. Naturally Occurring Polymers. In: Ravve A, editor. Principles of Polymer Chemistry. Boston, MA: Springer US. p. 449–475. [accessed 2019 Feb 6]. https://doi.org/10.1007/978-1-4615-4227-8_7.

Sadat Ebrahimi MM, Schönherr H. 2014. Enzyme-Sensing Chitosan Hydrogels. Langmuir. 30(26):7842–7850. doi:10.1021/la501482u.

Sarmento B, Ribeiro A, Veiga F, Sampaio P, Neufeld R, Ferreira D. 2007. Alginate/Chitosan Nanoparticles are Effective for Oral Insulin Delivery. Pharm Res. 24(12):2198–2206. doi:10.1007/s11095-007-9367-4.

Sezer AD, Akbuğa J. 1995. Controlled release of piroxicam from chitosan beads. Int J Pharm. 121(1):113–116. doi:10.1016/0378-5173(94)00413-Y.

Shen M, Huang Y, Han L, Qin J, Fang X, Wang J, Yang VC. 2012. Multifunctional drug delivery system for targeting tumor and its acidic microenvironment. J Controlled Release. 161(3):884–892. doi:10.1016/j.jconrel.2012.05.013.

Shimotoyodome A, Kobayashi H, Tokimitsu I, Matsukubo T, Takaesu Y. 2006. Statherin and Histatin 1 Reduce Parotid Saliva-Promoted Streptococcus mutans Strain MT8148 Adhesion to Hydroxyapatite Surfaces. Caries Res Basel. 40(5):403–11.

Shu XZ, Zhu KJ. 2000. A novel approach to prepare tripolyphosphate/chitosan complex beads for controlled release drug delivery. Int J Pharm. 201(1):51–58. doi:10.1016/S0378-5173(00)00403-8.

Siqueira W. L., Custodio W, McDonald EE. 2012. New insights into the composition and functions of the acquired enamel pellicle. J Dent Res. 91(12):1110–1118. doi:10.1177/0022034512462578.

Siqueira WL, Dawes C. 2011. The salivary proteome: Challenges and perspectives. PROTEOMICS – Clin Appl. 5(11-12):575–579. doi:10.1002/prca.201100046.

Siqueira Walter L., Lee YH, Xiao Y, Held K, Wong W. 2012. Identification and characterization of histatin 1 salivary complexes by using mass spectrometry. PROTEOMICS. 12(22):3426–3435. doi:10.1002/pmic.201100665.

Siqueira WL, Margolis HC, Helmerhorst EJ, Mendes FM, Oppenheim FG. 2010. Evidence of Intact Histatins in the in vivo Acquired Enamel Pellicle. J Dent Res. 89(6):626–630. doi:10.1177/0022034510363384.

Sissons CH, Wong L, Shu M. 1998. Factors affecting the resting pH of in vitro human microcosm dental plaque and Streptococcus mutans biofilms. Arch Oral Biol. 43(2):93–102.

Souza M, Vaz A, Correia M, Cerqueira M, Vicente A, Carneiro-da-Cunha M. 2014. Quercetin-Loaded Lecithin/Chitosan Nanoparticles for Functional Food Applications. Food Bioprocess Technol. 7(4):1149–1159. doi:10.1007/s11947-013-1160-2.

Thandapani G, P. SP, P.n. S, Sukumaran A. 2017. Size optimization and in vitro biocompatibility studies of chitosan nanoparticles. Int J Biol Macromol. 104:1794–1806. doi:10.1016/j.ijbiomac.2017.08.057.

Tung MS, Eichmiller FC. 2004. Amorphous calcium phosphates for tooth mineralization. Compend Contin Educ Dent Jamesburg NJ 1995. 25(9 Suppl 1):9–13.

Valente MT, Moffa EB, Crosara KTB, Xiao Y, Oliveira TM de, Machado MA de AM, Siqueira WL. 2018. Acquired Enamel Pellicle Engineered Peptides: Effects on Hydroxyapatite Crystal Growth. Sci Rep. 8(1):3766. doi:10.1038/s41598-018-21854-4.

Vitorino R, Calheiros-Lobo MJ, Duarte JA, Domingues PM, Amado FML. 2008. Peptide profile of human acquired enamel pellicle using MALDI tandem MS. J Sep Sci. 31(3):523–537. doi:10.1002/jssc.200700486.

Wang Y, Li P, Tran TT-D, Zhang J, Kong L. 2016. Manufacturing Techniques and Surface Engineering of Polymer Based Nanoparticles for Targeted Drug Delivery to Cancer. Nanomaterials. 6(2):26.

Wong A, Subar PE, Young DA. 2017. Dental Caries: An Update on Dental Trends and Therapy. Adv Pediatr. 64(1):307–330. doi:10.1016/j.yapd.2017.03.011.

Xiao Y, Karttunen M, Jalkanen J, Mussi MCM, Liao Y, Grohe B, Lagugné-Labarthet F, Siqueira WL. 2015. Hydroxyapatite Growth Inhibition Effect of Pellicle Statherin Peptides. J Dent Res. 94(8):1106–1112. doi:10.1177/0022034515586769.

Xiong M, Li Y, Bao Y, Yang X, Hu B, Wang J. 2012. Bacteria-Responsive Multifunctional Nanogel for Targeted Antibiotic Delivery. Adv Mater. 24(46):6175–6180. doi:10.1002/adma.201202847.

Yang X, Grailer JJ, Pilla S, Steeber DA, Gong S. 2010. Tumor-Targeting, pH-Responsive, and Stable Unimolecular Micelles as Drug Nanocarriers for Targeted Cancer Therapy. Bioconjug Chem. 21(3):496–504. doi:10.1021/bc900422j.

Zhang J, Tang Q, Xu X, Li N. 2013. Development and evaluation of a novel phytosome-loaded chitosan microsphere system for curcumin delivery. Int J Pharm. 448(1):168–174. doi:10.1016/j.ijpharm.2013.03.021.

Zhang N, Li Jiahui, Jiang W, Ren C, Li Jianshu, Xin J, Li K. 2010. Effective protection and controlled release of insulin by cationic beta-cyclodextrin polymers from

alginate/chitosan nanoparticles. Int J Pharm. 393(1–2):212–218. doi:10.1016/j.ijpharm.2010.04.006.

Zheng B, Karski M, Taylor SD. 2019. Thermoresponsive hydroxybutylated starch nanoparticles. Carbohydr Polym. 209:145–151. doi:10.1016/j.carbpol.2019.01.021.

Zimmerman JN, Custodio W, Hatibovic-Kofman S, Lee YH, Xiao Y, Siqueira WL. 2013. Proteome and Peptidome of Human Acquired Enamel Pellicle on Deciduous Teeth. Int J Mol Sci. 14(1):920–934. doi:10.3390/ijms14010920.

Chapter 2

2 A pH-sensitive Delivery System for the Prevention of Dental Caries Using Salivary Proteins

2.1 Introduction

Saliva is a complex fluid composed of proteins, enzymes, and a variety of electrolytes. Many physiological functions, such as chewing, initial digestion of food, wetting and lubrication are regulated by saliva (Humphrey and Williamson 2001; Siqueira and Dawes 2011). It also plays an active role in oral homeostasis, including partial protection against microbial activities, the maintenance of both salivary pH and tooth integrity (Mandel 1987). The concentration of proteins present in the saliva can be used as an indicator to monitor oral health, as the severity and occurrence of oral diseases have been associated with composition and quantitative changes in salivary proteins (Scarano et al. 2010). Many of the salivary proteins are active in the regulation of tooth homeostasis, either by directly exerting antimicrobial effects or interference in regard to microbial colonization. Examples include statherin, histatins (HTNs), defensins, lactoferrin and mucin (Hemadi et al. 2017) .

In particular, the HTN are of great interest because these proteins are multifunctional. They have demonstrated biological functions including the inhibition of calcium and phosphate precipitation on enamel and antimicrobial activities which are directly related to the regulation of oral homeostasis (Oppenheim et al. 2007; Siqueira et al. 2010; Siqueira et al. 2012). The HTNs mainly consist of HTN1, HTN3, and HTN5, which have molecular weights of 4929, 4063, and 3037 Dalton respectively. Each supplies about 20-30% of the total HTN pool (Gusman et al. 2004). HTN1 is the only phosphorylated HTN (McDonald et al. 2011) and previous studies have demonstrated its effectiveness in reducing bacterial colonization on tooth surfaces (Shimotoyodome et al. 2006; Vitorino et al. 2008). HTN5 has the most potent antifungal activity against *Candida albicans*, which is a pathogenic yeast (Puri and Edgerton 2014). HTN3 was demonstrated to be the most effective in killing against *Streptococcus mutans (S. mutans)* (Basiri et al.

2017), which is commonly found in the oral cavity and is a significant contributor towards dental caries.

These proteins are often present in low concentrations (Fábián et al. 2012) inside the oral cavity due to the high proteolytic activity of saliva (Helmerhorst et al. 2006). Therefore, we proposed a delivery system to load and protect these proteins for their use as inhibitors of tooth decay. The use of stimulus-responsive polymeric nanoparticles synthesized from natural polymers has recently gained substantial attention, as such smart delivery systems have the potential to improve the overall colloidal stability of the loaded molecules and modulate pharmacokinetics, often resulting in reduced toxicity and enhanced efficacy (Mihu et al. 2010; Yang et al. 2010; Shen et al. 2012; Xiong et al. 2012). The loaded cargo can be released in a stimulus-responsive manner. Examples of stimuli include changes in pH, ionic strength, temperature, UV light, magnetic field or the presence of specific biological molecules (Lee et al. 2003; Basel et al. 2011; Chen et al. 2014; Fan and Gillies 2017). In particular, for applications involving the delivery of drugs to the oral cavity. It would be ideal for the delivery system to remain stable at physiological salivary pH and selectively release the loaded cargo under acidic conditions. The pH-responsive property is crucial because the oral environment acidifies following carbohydrate intake, as a result of the consumption of food and beverages. These are the conditions which promote major oral disorders such as dental caries and dental erosion (Nikaido et al. 2004).

Many polymer-based materials have been studied for applications in controlled drug delivery, including naturally-occurring biopolymers. For instance, chitosan is a copolymer composed of *N*-acetyl-D-glucosamine and β(1-4) linked D-glucosamine (Dash et al. 2011). It is mainly obtained through the deacetylation of chitin under alkaline conditions (Raafat and Sahl 2009). Chitin is a biopolymer found in the exoskeletons of crustaceans, insects, and some fungi. (Tang et al. 2015). As the only known naturally occurring polycationic polysaccharide and with its ability to interact with anionic molecules, chitosan and its derivatives have been studied extensively for applications in the agricultural, medicinal and pharmaceutical industries (Souza et al. 2014; Bugnicourt and Ladavière 2016; Olivera et al. 2016).

Previous studies have utilized chitosan in toothpaste as an antimicrobial agent due to its broad antimicrobial spectrum, covering both Gram-negative and Gram-positive bacteria as well as fungi (Carvalho and Lussi 2014; Costa et al. 2014). Aside from its antimicrobial effect, chitosan also offers other advantages including biodegradability (Kean and Thanou 2010) and biocompatibility (Thandapani et al. 2017). It also exhibits pH-dependent solubility due to the presence of amino groups on the polymer chains (Cha et al. 2006). The functional amino groups can serve as platforms for interactions with other anionic molecules to form nanoparticles, where the choice of anionic molecules depends on the intended applications. The resulting nanoparticles should have small particle diameters (~200 nm) to ensure a high surface area to volume ratio. Size distribution, also known as the polydispersity index (PDI) of the nanoparticles should also be minimized (< 0.3) to obtain a uniform size distribution. Colloidal stability is equally as important, and it is directly related to the surface charge (zeta potential) of the nanoparticles. These parameters will be measured by dynamic light scattering (DLS), which measures the Brownian motion of small particles in suspension and relates it to the size of the particles. The particles will be illuminated by a laser and the intensity fluctuations in the scattered light will be analyzed to determine particle size.

In the current work, we propose pH-sensitive chitosan nanoparticles (CNs) for salivary proteins delivery. We hypothesized that salivary protein-loaded CNs can i) selectively release the loaded proteins under low pH environments, ii) offer protection against proteolysis at the physiological salivary pH, and iii) reduce *S. mutans* biofilm formation on hydroxyapatite. To test these hypotheses, HTN3 was selected as the target protein, and our objectives were to: 1) optimize CN formulation via ionic gelation with four different types of chitosan polymers; 2) characterize both blank and HTN3-loaded CNs; 3) quantify loading and release profiles of HTN3; 4) assess the protection offered by loading against enzymatic degradation in 10-fold diluted human saliva; 5) evaluate the effectiveness of HTN3-loaded CNs in reducing *S. mutans* biofilm formation on hydroxyapatite discs.

2.2 Materials and Methods

Materials

Ultra-low molecular weight (MW) chitosan and low MW chitosan (2) were purchased from Glentham Life Sciences (Corsham, UK). The other low MW chitosan (1), medium MW chitosan, and ZipTip C18 pipette tips were acquired from Millipore Sigma (Oakville, ON). All filters, including Acrodisc 0.45 and 0.2 μm syringe filters with Supor Membrane and 10k Dalton Nanosep filters were purchased from Pall Corporation (Mississauga, ON). HTN3 was acquired from Synpeptide Co., Ltd. (Shanghai, China). *S. mutans* UA159 was kindly donated by the University of Toronto (Toronto, ON). Hydroxyapatite discs with 5 mm diameter and 2 mm thickness were obtained from Clarkson Chromatography Products Inc. (South Williamsport, PA). Bicinchoninic acid assay kit was acquired from Thermo Fisher Scientific (Mississauga, ON). All other chemicals, including sodium tripolyphosphate (TPP), were purchased from Millipore Sigma (Oakville, ON).

Table 2.1 Summary of different types of chitosan polymers.

Type	MW (Dalton)	Degree of Deacetylation
Medium	190,000 – 310,000	75 – 85%
Low (2)	250,000 (Average)	91%
Low (1)	50,000 – 190,000	75 – 85%
Ultra-Low	20,000 (Average)	91%

Optimized CNs Preparation

Unloaded CNs. CNs were prepared by a modified version of the ionic gelation procedure described previously (Calvo et al. 1997). Preliminary work that studied the effect of chitosan molar mass and degree of acetylation (Table 2.1), pH of chitosan/TPP solutions, and chitosan to TPP ratios on CN characteristics was performed to optimize CN synthesis as follows. 100 mg of ultra-low MW chitosan was dissolved in 100 mL of 0.4% v/v concentrated HCl. The pH of the chitosan solution was adjusted to 5.9 with 1 M NaOH, then filtered using a 0.45 μm syringe filter. 100 mg of TPP was dissolved in 100 mL of Millipore water, its pH was adjusted to 6.0 and it was filtered through a 0.22 μm syringe filter. 0.36 mL of TPP solution was added dropwise into 2.5 mL of chitosan solution under constant stirring at 700 rpm, such that the mass ratio of chitosan to TPP is 6.94:1.

Preparation of HTN3-loaded CNs. HTN3 was mixed with chitosan solution before ionic gelation with TPP. 0.29 mL of the 0.1% w/v TPP solution was introduced dropwise into 2 mL of 0.1% w/v chitosan and 0.0025% w/v HTN3 under constant stirring at 700 rpm. The loading ratio of chitosan to HTN3 by mass was 40:1, and 0.45 mL of the suspension contained 10 μg of HTN3. HTN3 loading ratios could be changed to load more or less HTN3 as needed. Each preparation was performed in triplicate.

Characterizations of CNs

DLS. Particle diameter, PDI and zeta potential were measured by DLS (Smoluchowski equation, wavelength of 630 nm at 25°C) using a Malvern Zetasizer Nano ZS instrument (Malvern Instruments Ltd, Malvern UK). 1 mL of the CNs suspension was loaded into a disposable polystyrene cuvette for particle size and polydispersity index measurement. 0.75 mL of the same suspension was injected into a folded capillary cell for zeta potential measurement. Measurements were performed in triplicate.

Transmission electron microscopy (TEM). The morphology of the CNs was visualized by TEM with the Philips CM10 (Philips, Amsterdam, Netherlands) at 80 kV. To remove salts, 3 mL of the CNs suspension was loaded into a 50 kg/mol MW cut-off regenerated

cellulose dialysis tubing (Spectrum Labs, New Brunswick, NJ) and dialyzed in 1 L of deionized water for 3 hours under constant stirring. TEM samples were prepared by placing one drop of the dialyzed CNs suspension onto the Formvar®-coated copper grid, and the sample was dried overnight under an air atmosphere. Images were captured in triplicate.

pH-dependent swelling. To investigate the pH-dependence of CN size, initial particle size measurements were taken at a starting pH of 6.3 (time = 0 minutes). The pH of the suspension was then adjusted to different pH values: 3, 4 and 5 directly with 1 M HCl. After the pH adjustments, particle size, PDI and zeta potential were observed by DLS at 10, 20, 30, 60, 120, and 240 minutes in triplicate at each pH value. The CNs were not re-suspended in buffers due to possibility of salt accumulation.

Stability. CNs were stored at 4°C for 61 days to evaluate colloidal stability. Particle size and zeta potential were measured by DLS on days 1, 10, 15, 22, 30, 35, 45, 52, and 61 in triplicate.

Loading and Release of HTN3

pH-dependent release study. 0.05 mL of pH 6.8, 25 mM phosphate buffer/500 mM NaCl solution was added to 0.45 mL of HTN3-loaded CNs. The 0.5 mL suspension was then centrifuged at 14462 g for 10 minutes using a 10 kg/mol cut-off Nanosep filter. Only the free HTN3 (4063 Dalton) is small enough to pass through the filter. The filtrate was collected to determine loading efficiency by gel electrophoresis. The pH of the retentate on top of the filter was adjusted to pH 3, 4, or 5 using 1 M HCl and incubated at 37°C for 30 minutes. The suspension was centrifuged again, allowing the passage of released HTN3 through the filter. Subsequently, the filtrate was collected to determine the extent of protein release. Both loading and release filtrates, and a HTN3 standard of 5 μg were vacuum dried. The release study was performed in triplicate.

Cationic polyacrylamide gel electrophoresis (PAGE). Cationic-PAGE was performed as previously described (Siqueira et al. 2010). Lyophilized samples were dissolved in sample loading buffer composed of 0.04% w/v methyl green and 20% w/v sucrose.

Electrophoresis separation was performed at a constant voltage of 120 V. Subsequently, the gels were stained overnight with 0.1% w/v coomassie-blue dye in 7% v/v acetic acid and 8% v/v methanol. The following day, the gels were de-stained with 40% v/v methanol and 10% v/v acetic acid.

Loading Efficiency. HTN3-loaded CNs with 2%, 5%, and 10% w/w (HTN3 to chitosan) loading ratios were prepared as previously described with modifications to the mass ratio of chitosan to HTN3. 0.05 mL of pH 6.8, 25 mM phosphate buffer/500 mM NaCl solution was added to 0.45 mL of HTN3-loaded CNs at each loading ratio. The 0.5 mL suspension was then centrifuged at 14462 g for 10 minutes using a 10,000 g/mol cut-off Nanosep filter. Since the un-loaded HTN3 (4063 Dalton) is small enough to pass through the filter, the filtrate could be used to calculate loading efficiency. The filtrate was collected, and vacuum dried together with a HTN3 standard of 5 μg for use as control. Cationic-PAGE was performed as described previously. The loading efficiency was determined by Image Lab (BioRad) via relative quantity tool. The relative quantity is the ratio of the band volume and intensity divided by the reference band volume and intensity. A HTN3 standard band was set as the reference and the other bands were compared against the reference band. The loading experiment was performed in triplicate for each loading ratio.

Cumulative Release. HTN3-loaded CNs were prepared as previously described. 0.05 mL of pH 6.8, 25 mM phosphate buffer/500 mM NaCl solution was added to 0.45 mL of HTN3-loaded CNs. The 0.5 mL suspension was then centrifuged at 14462 g for 10 minutes using a 10 kg/mol cut-off Nanosep filter. Retentate on top of the filter was kept constant at 6.8 or adjusted to pH 3, 4, or 5 using 1 M HCl, then incubated at 37°C for 30 minutes. It was then subjected to centrifugal ultrafiltration at 14462 g for 10 minutes to separate the released protein. Subsequently, the filtrate was collected. The retentate was replenished back to 0.5 mL with the buffer at the same pH. The filtrate and a HTN3 standard of 5 μg were analyzed by PAGE as previously described. The separation and quantification of released protein was repeated at 30, 60, 90, 120, 150, 180, and 210 minutes. Cumulative release was performed in triplicate at each pH value.

pH Cycling Release. pH of HTN3-loaded CNs was cycled between pH 4 and 6.8 to reflect pH changes in the oral cavity. 0.05 mL of pH 6.8, 25 mM phosphate buffer/500 mM NaCl solution was added to 0.45 mL of HTN3-loaded CNs. The 0.5 mL suspension was then centrifuged at 14462 g for 10 minutes using a 10 kg/mol cut-off Nanosep filter. The remaining retentate on top of the filter was adjusted to pH 4 with 1 M HCl and subjected to centrifugal ultrafiltration at 14462 g for 10 minutes to separate the released protein. The filtrate was collected and the retentate was replenished with pH 6.8 buffer to a volume of 0.5 mL. The pH cycling release followed the adjustments order of pH 4, 6.8, 4, 6.8, 4, 6.8, 4. Cationic-PAGE was performed on all filtrates and a HTN3 standard of 5 μg as previously described. pH cycling was performed in triplicate.

Protein Degradation Study

Saliva Collection. Whole saliva samples were collected 2 hours after breakfast between 9:00 am to 11:00 am to minimize the effect of circadian rhythm. Samples included 3 healthy participants ranging from 24 to 32 years old. Stimulated whole saliva was obtained by masticating on a piece of parafilm. 3 to 5 mL of saliva was collected on ice. Immediately after collection, whole saliva samples were centrifuged for 10 minutes at 14462 g at 4 °C to separate the bacteria, cells and other debris. The supernatant is referred to as whole saliva supernatant (WSS). Salivary proteins were quantified using a bicinchoninic acid assay kit.

Degradation of Free HTN3 in WSS. The degradation experiments were carried out in 10-fold diluted WSS. 50 μg of free HTN3 was added to diluted WSS (100 mg salivary protein/mL) in a final volume of 1 mL. The pH was adjusted to 6.8 using 1 M HCl or 1 M NaOH, depending on the pH of collected saliva. An aliquot of 100 μL was collected and boiled for 5 minutes to terminate proteolytic activity after incubation at 37 °C for 0, 0.5, 1, 2, 3 or 6 hours. Samples were dried and desalted. Cationic-PAGE was performed to study the degradation samples. The extent of degradation was quantified by Image Lab using the relative quantity tool.

Degradation of HTN3-loaded CNs in WSS. The degradation experiments were carried out with 10-fold diluted WSS. 0.5 mL of the HTN3-loaded CNs (containing 50 μg of HTN3) was added to diluted WSS (100 mg salivary protein/mL) to reach a final volume of 1 mL. The final pH was standardized to 6.8 with 1 M HCl or 1 M NaOH, depending on the initial pH of saliva. An aliquot of 100μL was collected after incubation at 37°C at the following time points: 0, 0.5, 1, 2, 3 and 6 hours. The pH was adjusted to 3 to release all of the HTN3 within the delivery system. After centrifugation with a 10,000 g/mol Nanosep filter, the filtrate was retrieved and boiled for 5 minutes to terminate proteolytic activity. Samples were dried and desalted, followed by Cationic-PAGE. The extent of degradation was quantified by Image Lab through relative quantity tool. Each degradation study was performed in triplicate.

S. mutans Killing Assay and Biofilm Formation

S. mutans Growth. 10 colonies of *S. mutans* (UA 159) were grown for 14 hours in 10 mL of Tryptone Yeast Extract Broth (TYEB) supplemented with 1% glucose at 37 °C and 10% CO_2. After incubation, the bacterial suspension was washed with 0.9% NaCl twice and the supernatant was discarded after each wash. The pellet was resuspended in 1.2 mL of phosphate-buffered saline (PBS). 0.8 mL of the suspension were used for optical density (OD) measurement at 600 nm, then diluted with PBS if needed to obtain a reading of approximately 1.5, corresponding to the bacterial concentration of 10^9 colon forming units (CFU)/mL based on the calibration curve.

Killing Assay. From the suspension with 1.5 OD reading, 0.1 mL was added to 9.9 mL of PBS to obtain a bacterial concentration of 10^7 CFU/mL. 50 μL of the 10^7 CFU/mL suspension was added to an equal volume of a serial dilution series of HTN3 in a 96-well polypropylene microtiter plate. The samples were then incubated at 37 °C for 1.5 hours. After incubation, each sample was diluted 10^3 and 10^4-fold in PBS, and 20 μL of each dilution was plated onto Todd Hewitt Broth (THB) agar plates. Bacterial viability was assessed by colony counting using comparisons against control samples incubated without

HTN3. The IC_{50} value was calculated based on the dose-response curve. The killing assay was performed in triplicate.

S. mutans Biofilm Formation on Hydroxyapatite Discs. Hydroxyapatite discs were fixed on the interior of a 24-well polypropylene microtiter plate cover, where the discs were carefully positioned so that the plate cover fits both 24 and 96-well plates. The plate cover was placed to immerse all discs in a 96-well plate filled with 200 μL of 5 different treatment solutions: control (PBS), 0.03 mg/ mL HTN3, 0.1% w/v unloaded CNs, 0.1% w/v CNs containing 6 μg of loaded HTN3, and 12300 ppm fluoride solution for two hours. Three discs were assessed per treatment group. Subsequently, the plate cover was placed on a 24-well plate with 2 mL of 0.9% w/v NaCl to wash the discs. Afterwards the discs were immersed into 2 mL of TYEB supplemented with 1% w/v glucose and 10^7 CFU/mL of bacteria. The discs were then incubated at 37°C in 10% CO_2 for 8 hours. After incubation, the discs were washed again with NaCl, followed by further incubation for 16 hours immersed in 2 mL of TYEB supplemented with 0.1 mM glucose. Over the next 4 days, the discs were incubated in a repeating cycle between solution 1 and 2 where solution 1 is TYEB supplemented with 1% w/v sucrose for 8 hours, and solution 2 is TYEB supplemented with 0.1 mM glucose for 16 hours. On the 6^{th} day, all discs were transferred to separate tubes filled with 1 mL of PBS, followed by sonication to remove the biofilms off the discs. 0.5 mL of the suspension was transferred to pre-weighed tubes and centrifuged at 14400 g for 5 minutes. The supernatant was removed, and the weight of wet biofilm was measured. The same suspension was diluted 10^6 and 10^7 times in PBS, and 20 μL of each dilution was plated onto THB agar plates. Bacterial viability was assessed by colony counting. This experiment was performed with a sample size of 6.

Statistical Analyses

Statistical analyses were performed using software Prism 7.0 GraphPad. Biofilm mass and bacterial viability were analyzed by ordinary one-way ANOVA followed by Tukey's multiple comparisons test between each treatment group. The level of significance (α) was set at 0.05 (95% confidence interval).

2.3 Results

2.3.1 Optimization of CN Formulation

Chitosan samples with different MWs and degrees of acetylation were investigated initially to determine which would provide the best particles. We sought a diameter of less than 200 nm, a zeta potential of > 15 mV to afford colloidal stability, and a low polydispersity index of < 0.3 to have well-defined materials.

Medium MW. The effect of chitosan to TPP mass ratio was studied by varying the mass ratio from 3.5:1 to 10:1. The particle diameter decreased up to a ratio of 3.7:1, then increased (Figure 2.1a). The PDI followed a similar trend with an initial decrease in PDI up to 3.7:1 chitosan:TPP, followed by an increase at higher ratios (Figure 2.1b). Lastly, as shown on Figure 2.1c, zeta potential increased steadily with a corresponding increase in chitosan to TPP ratio. This was expected due to increased cationic polymer presence in the CNs. Taking all three parameters into consideration, the optimal formulation for medium MW chitosan was at the mass ratio of 4.17:1 (chitosan:TPP). Nanoparticles at this ratio had a diameter of 188 ± 2 nm in diameter, a PDI of 0.275 ± 0.007, and a zeta potential of 18 ± 3 mV.

Low MW (1). Similar trends were observed in low MW chitosan (1). Particle diameter and PDI continued to decrease with an increase in chitosan:TPP mass ratio until 5:1. Zeta potential increased as chitosan:TPP increased due to increased cationic polymer presence. The optimum formulation was chosen at 5.88:1 chitosan to TPP with a size of 160 ± 10 nm in diameter, a PDI of 0.28 ± 0.01, and a zeta potential of 17.9 ± 0.5 mV.

Low MW (2). Similar to the previous chitosan polymers, low MW (2) chitosan demonstrated the same trend. Particle diameter and PDI continued to decrease with a corresponding increase in chitosan:TPP until the ratio of 6.94:1. Zeta potential increased steadily as chitosan:TPP increased because of the presence of increased amount of cationic chitosan. The optimal ratio was selected at 6.94:1 chitosan to TPP. At this ratio, the resulting nanoparticles had a diameter of 320 ± 16 nm, a PDI of 0.39 ± 0.02, and a zeta potential of 23 ± 1 mV.

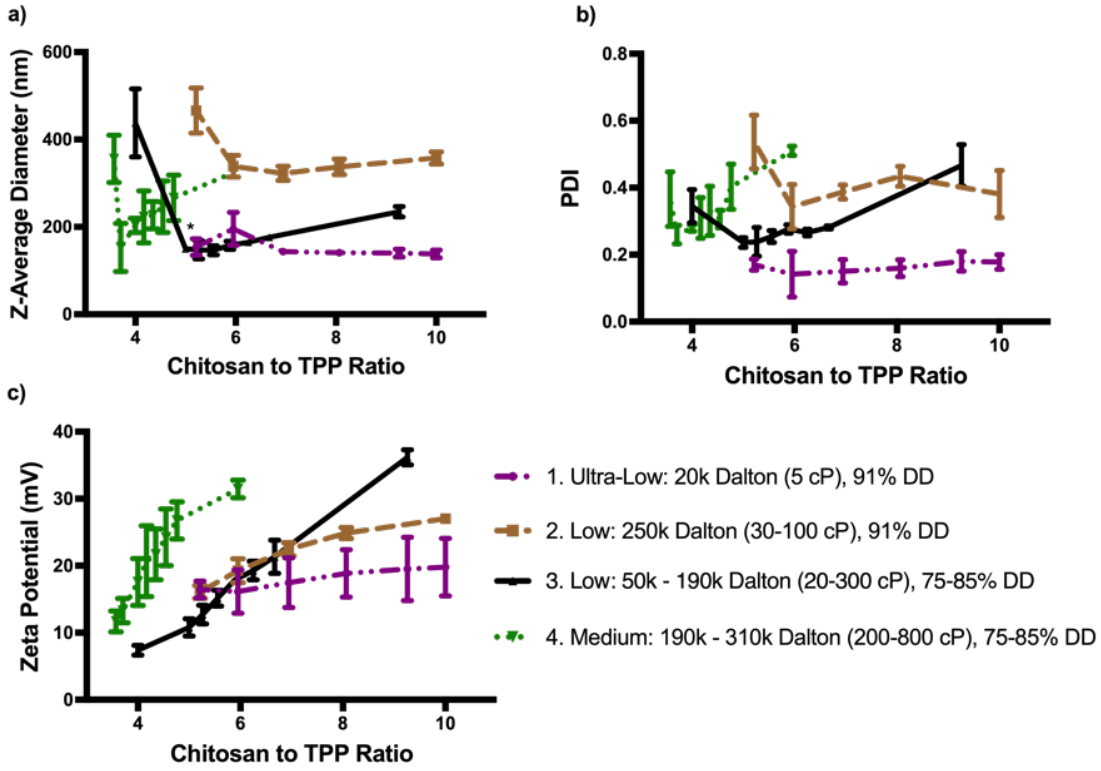

Figure 2.1 The effect of chitosan to TPP ratio on a) Z-average diameter. The particle diameter decreased when the ratio was increased until a certain threshold, beyond which particle diameter steadily increased. b) PDI followed a similar trend as particle diameter. c) Zeta potential increased with increasing chitosan:TPP ratio. Error bars correspond to the standard deviations of triplicate samples.

Ultra-low MW. Because of the lower MW and the higher degree of deacetylation, ultra-low MW chitosan was able to form nanoparticles across a wide range of chitosan to TPP mass ratios with similar particle diameters and PDI values. The optimal ratio was selected at 6.94:1 chitosan to TPP. At this ratio the nanoparticles had a diameter of 144 ± 6 nm, a PDI of 0.15 ± 0.04, and a zeta potential of 18 ± 4 mV. Ultra-low CNs were selected as the optimal formulation based on smallest particle diameter and lowest PDI at a relatively stable zeta potential.

2.3.2 Characterization of Unloaded and HTN3-loaded CNs by DLS

The CNs prepared from ultra-low MW chitosan were characterized by DLS. The unloaded CNs had a Z-average diameter of 144 ± 6 nm, a PDI of 0.15 ± 0.04, and a zeta potential of 18 ± 4 mV at pH 6.3, the pH of the initially prepared particle suspension. The protein of interest, HTN3, was loaded into the CNs at various loading ratios (Table 2.2). The HTN3-loaded particles had similar diameters, PDI, and zeta potential to the unloaded particles. Figure 2.2 shows the volume distribution of the HTN3-loaded CNs at pH 6.3 and at pH 3. At pH 3, the Z-average diameter increased to 260 nm, showing the pH-responsive swelling behavior of the CNs.

Table 2.2 DLS data for unloaded and HTN3-loaded CNs prepared from ultra-low MW chitosan. Error bars correspond to the standard deviations of triplicate samples.

Protein Loading Ratio (w/w%)	Z-Avg Diameter (nm)	PDI	Zeta (mV)
0 (unloaded)	144 ± 6	0.15 ± 0.04	18 ± 4
2	142 ± 6	0.16 ± 0.05	18 ± 2
5	134 ± 7	0.15 ± 0.03	19 ± 3
10	136 ± 6	0.16 ± 0.04	20 ± 3

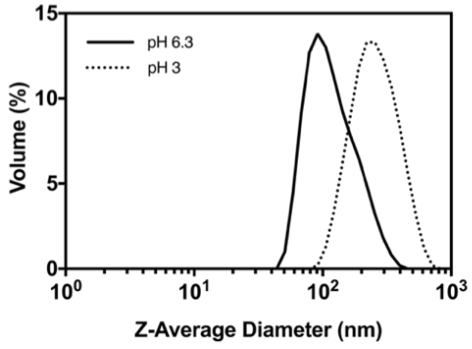

Figure 2.2 DLS volume distribution of blank CNs at pH 3 and pH 6.3 showing a representative increase in diameter at acidic pH due to swelling.

2.3.3 TEM Images of Unloaded and HTN3-loaded CNs

The CNs were then visualized with TEM. As shown in Figure 2.3, the CNs had a spherical morphology, and the observed diameters were in reasonable agreement with the data obtained from DLS.

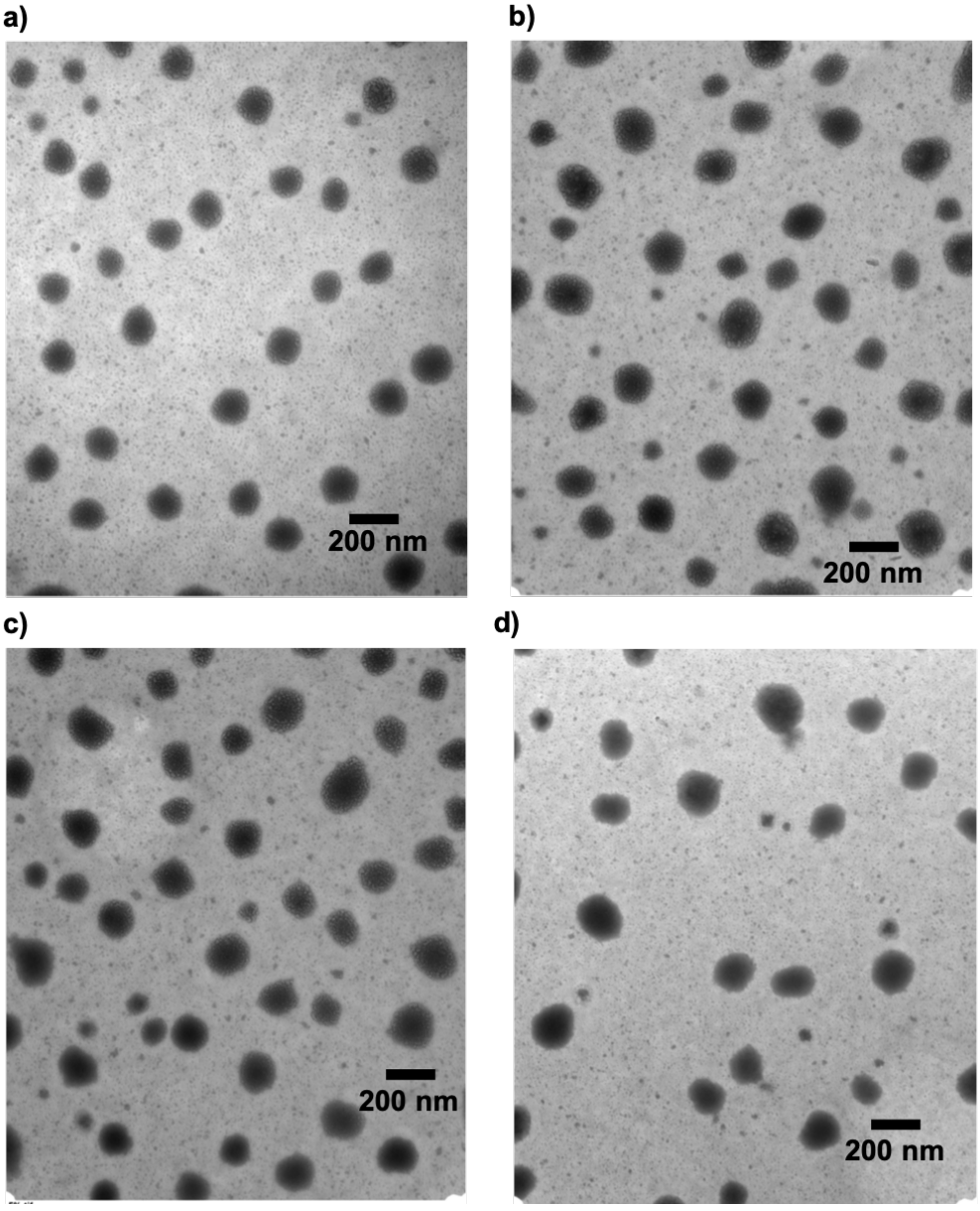

Figure 2.3 TEM images of CNs: a) Unloaded; b) HTN3-loaded at a 2% w/w loading ratio; c) HTN3-loaded at a 5% w/w loading ratio; d) HTN3-loaded at a 10% w/w loading ratio. The particles appeared spherical and the diameters were in reasonable agreement with the DLS results.

2.3.4 Stability of Unloaded CNs

The unloaded CNs were stored at 4 °C and DLS measurements were taken routinely over the course of 61 days. On day 1, the CNs had a particle diameter of 143 ± 4 nm, a PDI of 0.16 ± 0.02 at a zeta potential of 17.4 ± 0.4 mV. On day 61, they had a Z-average diameter of 152 ± 4 nm, a PDI of 0.16 ± 0.02 at a zeta potential of 17 ± 2 mV (Figure 2.4). These results indicate that the CNs are stable for at least 2 months when stored at 4°C.

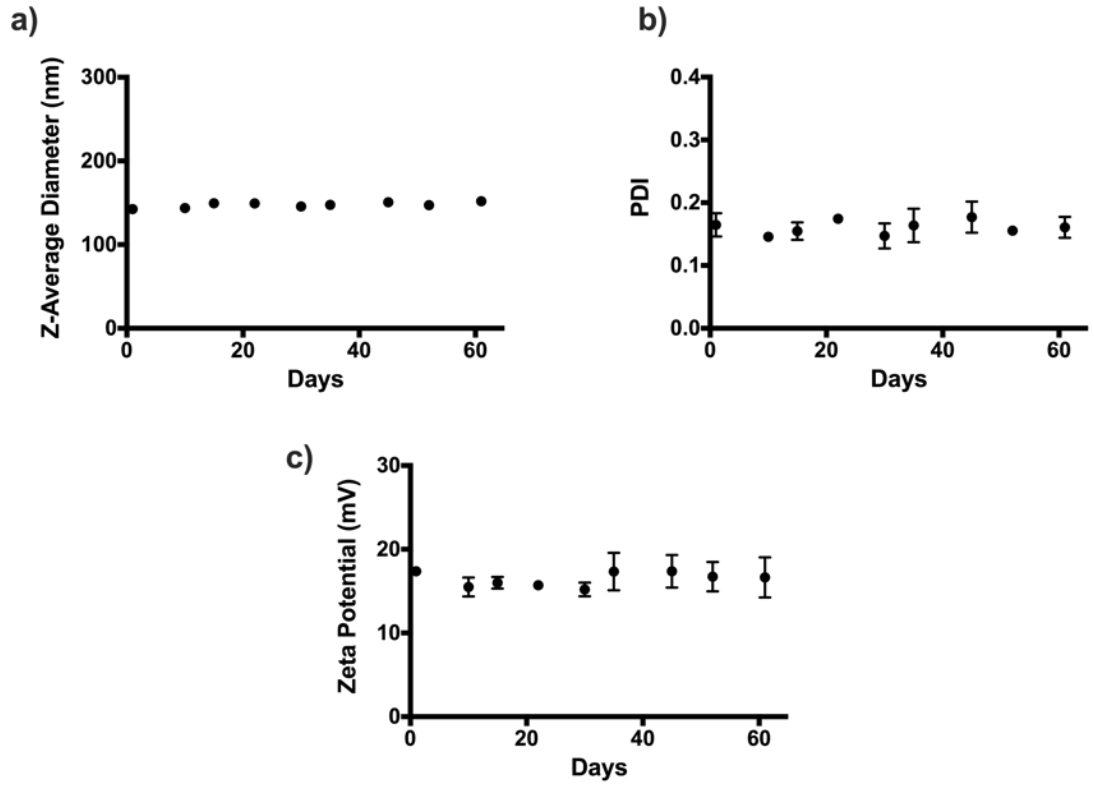

Figure 2.4 DLS data for CNs stored at 4°C for 61 days: a) Z-average diameter; b) PDI; c) Zeta potential. No changes were observed, suggesting that the nanoparticles are stable under these conditions. Error bars correspond to the standard deviations of triplicate samples. Some error bars are too small to be seen because the standard deviations are smaller than the data points.)

2.3.5 pH-dependent Swelling CNs

The pH-responsive properties of the unloaded CNs were examined first by adjusting the pH from the initial pH of 6.3 for the formulation to pH 3, 4, or 5. DLS measurements of the Z-average diameters at each pH indicated greater swelling at lower pH values (Figure 2.5a). The CNs swelled from 146 nm to 260 nm at pH 3. The swelling was rapid at each pH, reaching an equilibrium diameter at 10 minutes. We also subjected the CNs suspension to pH cycling between 6.3 to 4. Measurements of the Z-average diameter suggested that the CNs were able to selectively swell under acidic conditions and then to contract when the pH was increased upon removal of the stimulus (Figure 2.5b). However, there was a general trend towards larger diameters with repeated swelling cycles.

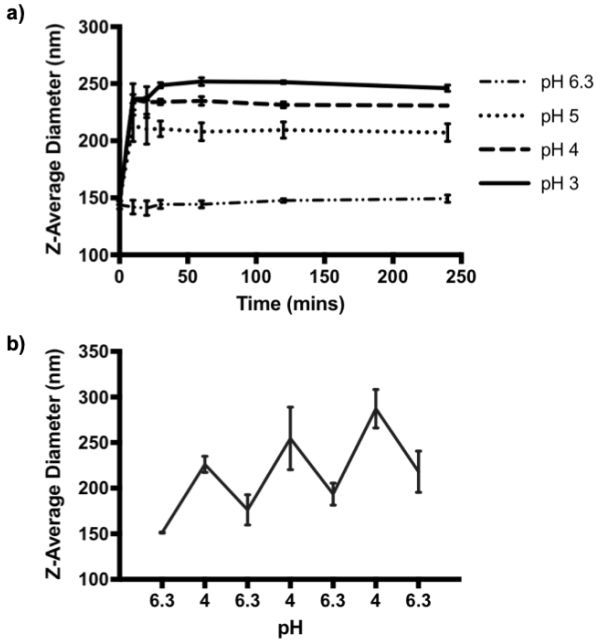

Figure 2.5 pH-responsive behavior of the CNs: a) Z-average diameters over time at different pH values from 3 to 6.3. The results suggest the degree of swelling is proportional to the acidity of the suspension. The swelling behavior was also rapid, and reached equilibrium 10 minutes after pH adjustment. b) The pH-responsive behavior was further examined through pH cycling between pH 6.3 and 4 at a 10-minute interval. The CNs were able to swell and contract accordingly based on the suspension pH. Error bars correspond to the standard deviations of triplicate samples.

2.3.6 Loading Efficiency

The protein of interest, HTN3 was loaded into CNs at three different loadings: 2, 5, and 10% w/w and after separation of the un-loaded protein by centrifugal ultrafiltration, it was quantified by Cationic-PAGE. The absence of protein bands shown on Figure 2.6 suggested that all of the HTN3 was successfully loaded into the CNs at each loading ratio.

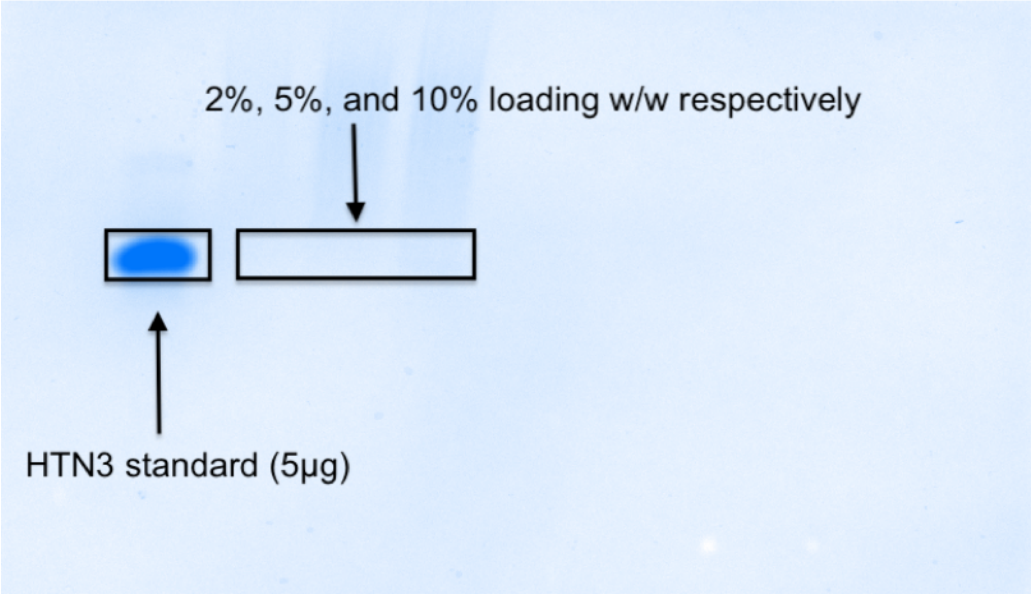

Figure 2.6 Loading ratios of 2%, 5%, and 10% w/w HTN3 to chitosan were investigated. The absence of the protein bands in the representative gel after isolation of unloaded protein by centrifugal ultrafiltration suggests the protein at each loading ratio was fully loaded into the nanoparticles. The experiment was repeated in triplicate.

2.3.7 pH-dependent Release of HTN3 from CNs

The release kinetics of HTN3-loaded CNs were investigated at different pH values over a period of 210 minutes, with protein release measured every 30 minutes. Figure 2.7a shows the Cationic-PAGE for the cumulative release at pH 3. For this particular experiment the CNs released ~90% of the loaded HTN3 over the 7 time points (210 minutes). pH cycling was also performed to reflect the pH changes that happen many times in the oral

cavity throughout the day. HTN3 loaded CNs were subjected to pH treatments in the following sequence: 6.8, 4, 6.8, 4, 6.8, 4, 6.8, and 4. After isolation of released protein and Cationic-PAGE at each pH change, protein bands of HTN3 were only observed at pH 4 and were absent at pH 6.8 (Figure 2.7b). This result shows the pH selective release for the CNs.

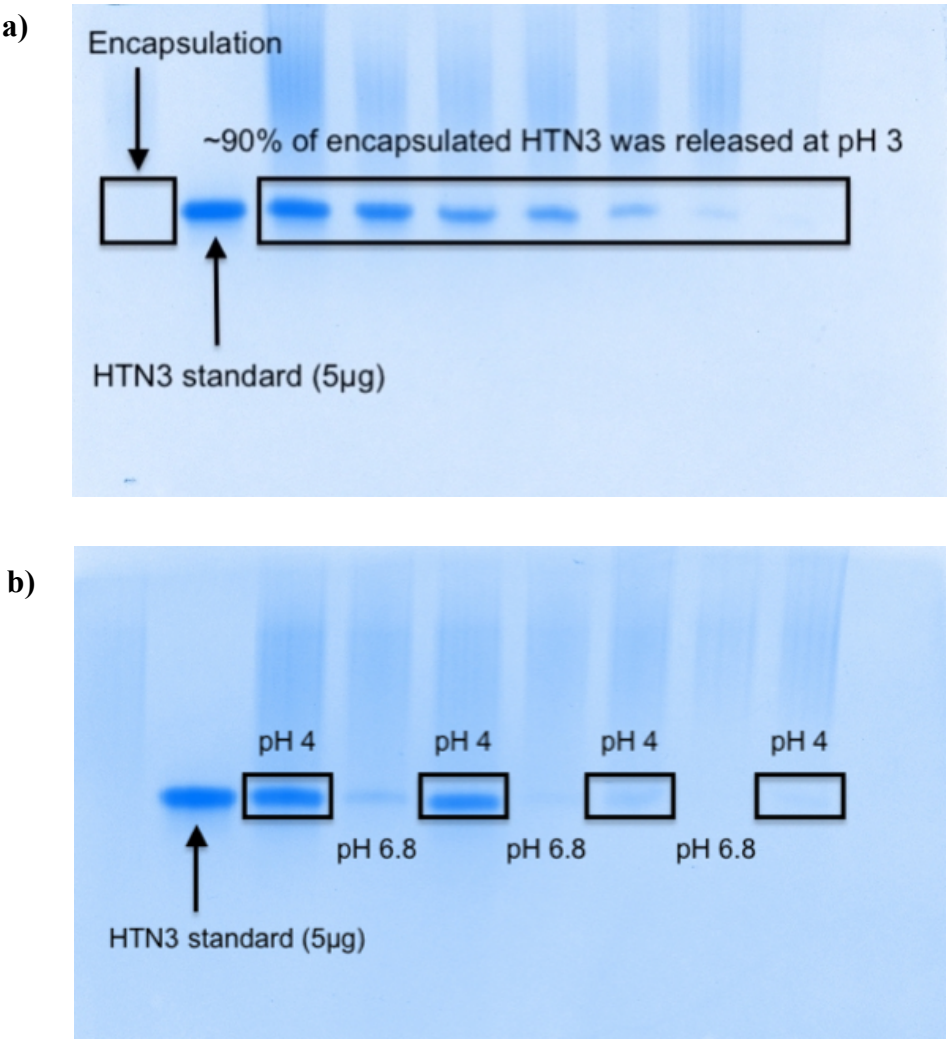

Figure 2.7 The cumulative and pH cycling release of HTN3-loaded CNs were investigated under different pH conditions with released protein displayed using Cationic-PAGE (representative example shown). a) Cumulative release at pH 3 over 7 time points obtained at 30-minute intervals. b) pH cycling from pH 4 to pH 6.8 at 30-minute intervals, showing that the CNs selectively released the loaded protein at pH 4 but not at 6.8. The experiment was repeated in triplicate.

The cumulative release experiment was repeated at pH 4, 5, and 6.8, the results were quantified using Image Lab and plotted in Figure 2.8a. The highest cumulative amount of HTN3 release was observed at pH 3, and there was minimal release at pH 6.8. On average, at pH 3, the CNs were able to release ~84 ± 7% of the loaded HTN3, ~58 ± 9% at pH 4, ~36 ± 3% at pH 5, and ~2 ± 2% at pH 6.8 over 7 separate releases. The pH cycling release was also quantified and presented in Figure 2.8b. The CNs were able to respond to the environmental pH changes and release the protein selectively at acidic pH.

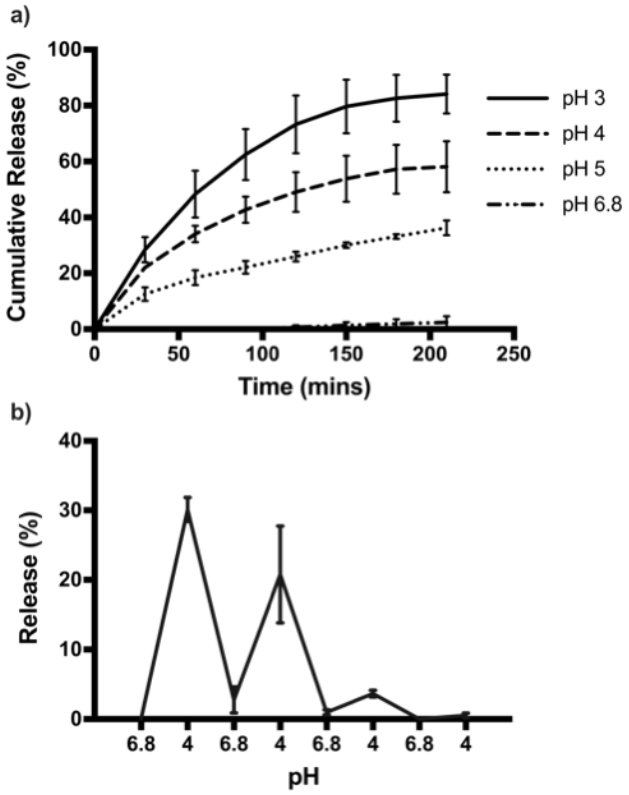

Figure 2.8 a) Release of HTN3 from CNs at different pH values were quantified using Image Lab. The highest extent of release and most rapid release was observed at pH 3, and there was minimal release at pH 6.8. On average, at pH 3, the CNs were able to release ~84 ± 7% of the loaded HTN3, ~58 ± 9% at pH 4, ~36 ± 3% at pH 5, and ~2 ± 2% at pH 6.8. b) pH cycling release at 30-minute intervals between pH 6.8 and 4 show that the CNs can adapt to environmental pH changes and release HTN3 selectively at pH 4 over 3 pH cycles. Error bars correspond to the standard deviations on triplicate samples.

2.3.8 HTN3 Degradation Study in WSS

In order to assess the protection offered through loading against enzymatic degradation in the oral cavity, a protein degradation study was conducted in 10-fold diluted human saliva to compare the degradation kinetics of free HTN3 and HTN3 loaded CNs. Figure 2.9a shows Cationic-PAGE for free HTN3 at different time points in contact with WSS. Figure 2.9b shows the Cationic-PAGE for HTN3 loaded into CNs. The protein bands of free HTN3 disappeared more rapidly, suggesting faster degradation without the protection offered by CNs.

a)

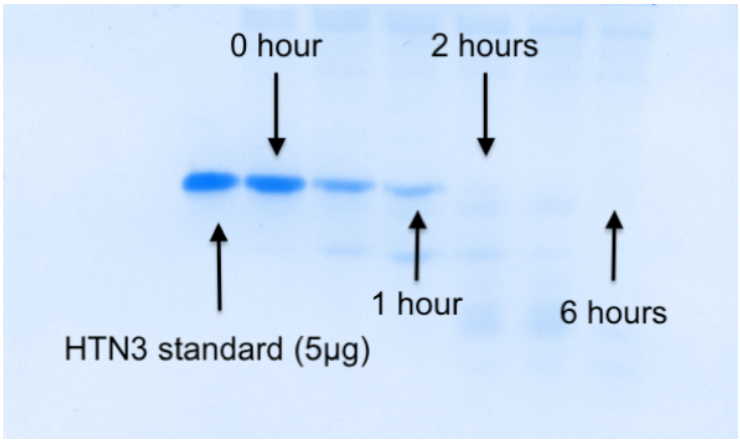

b)

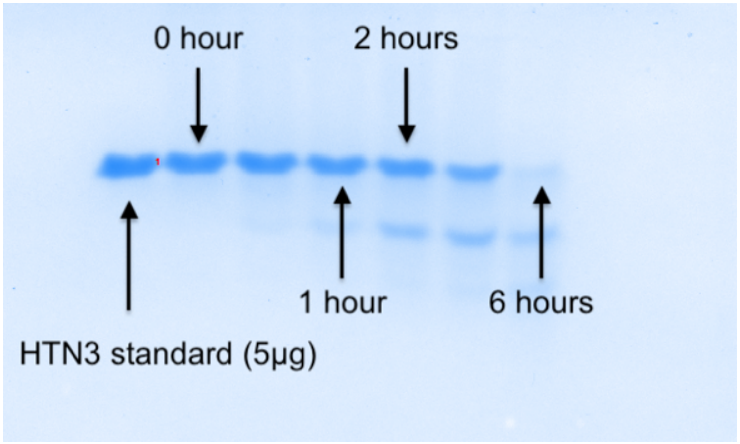

Figure 2.9 Protein degradation in WSS, evaluated by Cationic-PAGE (representative example shown, N = 3): a) free HTN3 and b) HTN3 loaded CNs. Most of the protein was degraded at the 2-hour mark for the control group, supported by the faded protein bands of HTN3. At the same time point, the protein band of HTN3 loaded within CNs remained relatively strong.

The degradation over time was quantified for both free HTN3 and HTN3 loaded CNs (Figure 2.10). For free HTN3, only 6 ± 5 % of the free HTN3 remained after 2 hours, whereas 47 ± 8 % of HTN3 was intact when it was loaded in the CNs delivery system. Protection provided by the CNs were plotted as the difference in degradation kinetic between free HTN3 and HTN3-loaded CNs.

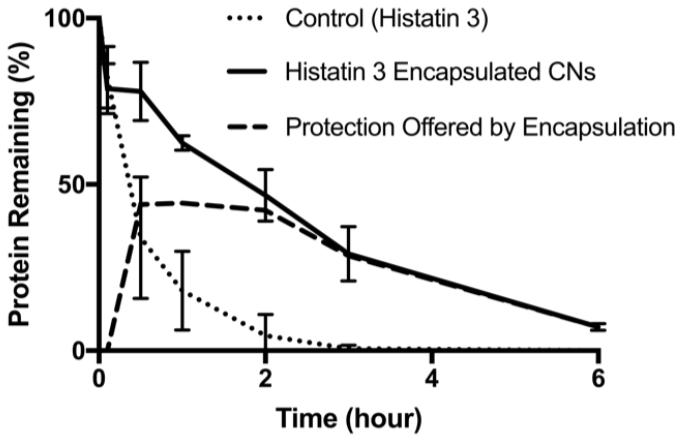

	Histatin 3 Remaining (%)	
Time (h)	Control	CNs
0	100	100
0.1	82 ± 9	79 ± 8
0.5	34 ± 18	78 ± 9
1	18 ± 12	63 ± 2
2	6 ± 5	47 ± 8
3	1 ± 1	29 ± 8
6	0	7 ± 1

Figure 2.10 Protein degradation over time for free HTN3 and HTN3-loaded into CNs. For free HTN3, most HTN3 was degraded in 2 hours. At the same time point, about half of HTN3 was still intact in the CNs delivery system. The dashed line represents the protection offered by the CNs, displayed as the difference in degradation percentage between free HTN3 and HTN3-loaded CNs. Error bars correspond to the standard deviations on triplicate samples.

2.3.9 *S. mutans* Killing Assay

To evaluate the effectiveness of HTN3 loaded CNs against biofilm formation by *S. mutans* on hydroxyapatite discs, the amount of HTN3 required to be loaded was first determined from a killing assay. First, a correlation was established between absorbance at 600 nm and colony-forming unit (CFU)/mL for *S. mutans*, where CFU is a unit commonly used in microbiology to estimate the number of viable bacterial cells in a given sample. This is shown in Figure 2.11, where a linear relationship between absorbance and CFU/mL was observed.

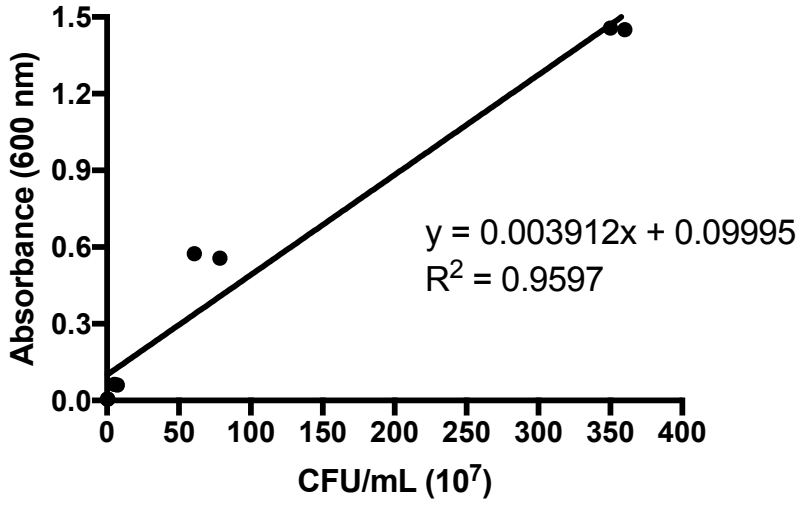

Figure 2.11 Relationship between optical absorbance at 600 nm and *S. mutans* CFUs. (N = 3), error bars cannot be seen because the standard deviations are smaller than the data points)

The antibacterial effect of pure HTN3 was evaluated through a killing assay against 10^7 CFU of *S. mutans*. 10^7 CFU was chosen because it is the bacterial population required to form a complete biofilm, and the IC_{50} was calculated to be 7.4 μM for pure HTN3 (Figure 2.12). IC_{50} is the concentration required to inhibit a biological process by half. The same concentration of HTN3 was used in the CN-loaded form for subsequent experiments and tested against biofilm formation of *S. mutans*.

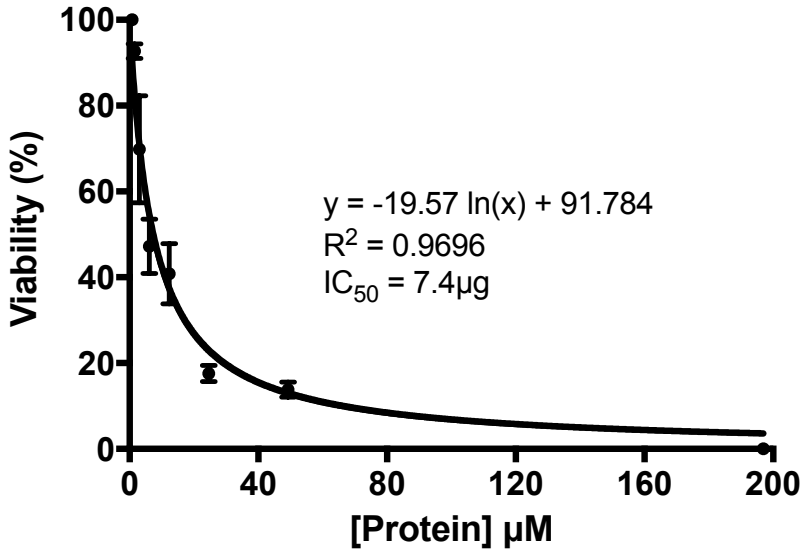

Figure 2.12 Killing assay results of pure HTN3 against 10^7 CFU *S. mutans*. Here, IC_{50} = 7.4 µM. Error bars correspond to the standard deviations on triplicate samples. Some error bars cannot be seen because the standard deviations are smaller than the data points (95% CI: 5.4 to 10.1 µM)

2.3.10 Biofilm Formation

Wet biofilm mass was measured to test the effectiveness of 4 different treatment groups including 7.4 µM HTN3, 0.1% w/v unloaded CNs, 7.4 µM HTN3 in CNs, and the gold standard 12300 ppm fluoride solution. They were compared against PBS as a control group. As presented in Figure 2.13, the control group had an average wet biofilm mass of 16 ± 2 mg, while the mass was 12 ± 1 mg for HTN3, 8 ± 2 mg for fluoride, 6 ± 1 mg for unloaded CNs, and 5.3 ± 0.9 for HTN3-loaded CNs.

Bacterial cell viability was also evaluated and presented in Figure 2.14. The PBS control led to 5.25 x 10^9 ± 1 x 10^8 CFU/mL of viable bacteria, while free HTN3 had 4.7 x 10^9 ± 0.2 x 10^9 CFU/mL, fluoride had 4.0 x 10^9 ± 0.4 x 10^9 CFU/mL, unloaded CNs had 3.0 x 10^9 ± 0.2 x 10^9 CFU/mL, and HTN3-loaded CNs had 2.3 x 10^9 ± 0.5 x 10^9 CFU/mL.

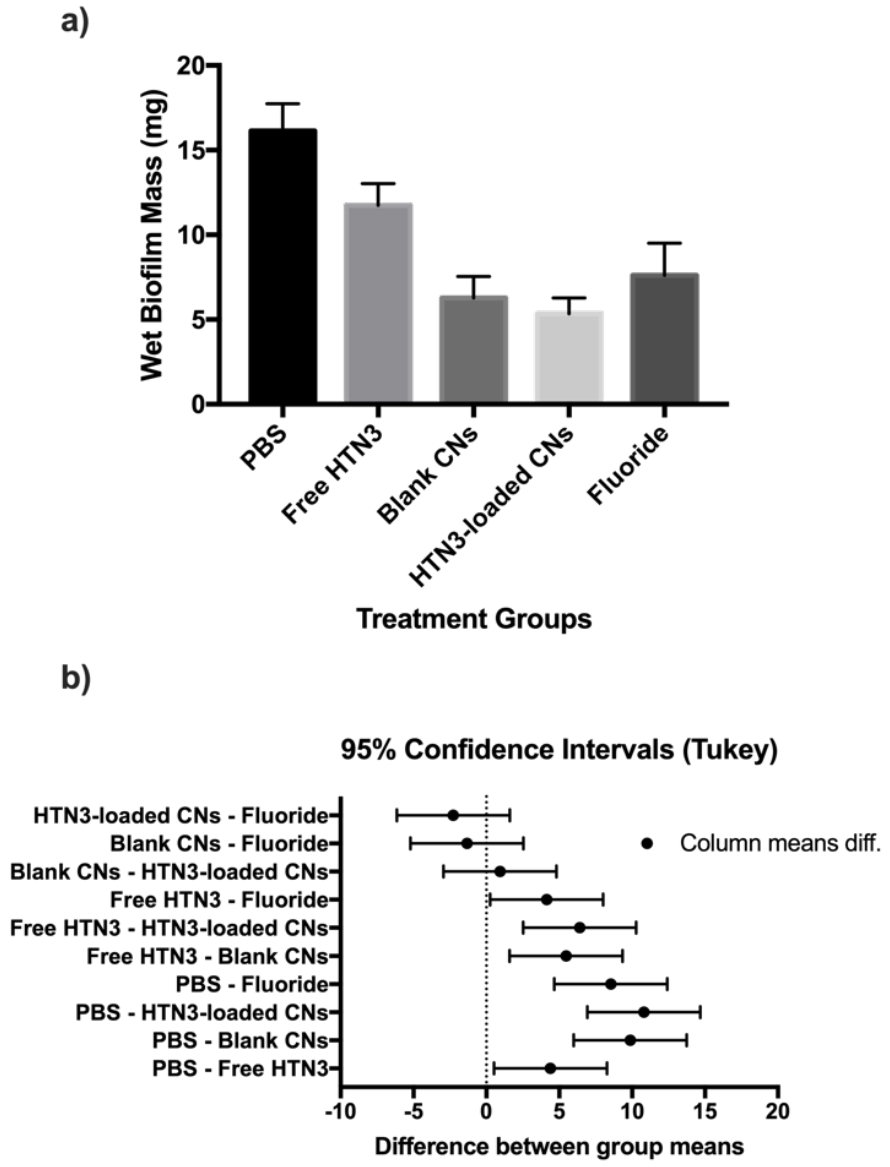

Figure 2.13 a) Wet biofilm masses for 4 treatment groups were compared against the control group PBS. All 4 treatment groups led to significantly lower biofilm mass than PBS. Fluoride, blank and HTN3-loaded CNs performed significantly better than free HTN3 in minimizing biofilm formation, but no significant difference in biofilm mass was observed between these treatment groups. Error bars correspond to the standard deviations on 6 samples. b) Tukey's multiple comparisons test was performed at 95% confidence intervals. The two groups were significantly different from each other only if the difference between group means ± upper and lower limits did not cross zero (dotted line).

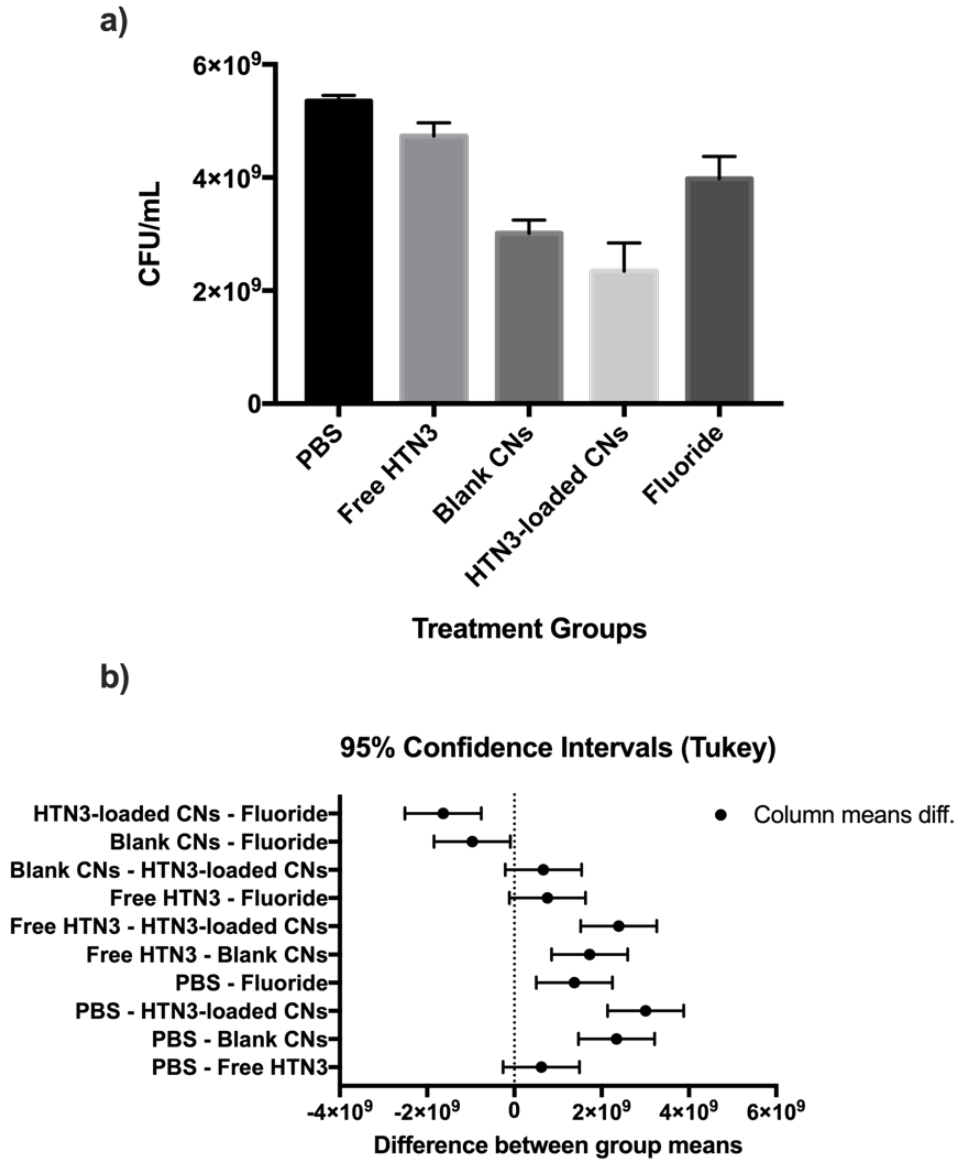

Figure 2.14 a) Bacterial viability for the 4 treatment groups were compared against the control group treated with PBS only. While free HTN3 did not control bacterial growth, fluoride treatment significantly decreased bacterial growth. Blank and HTN3-loaded CNs were the most effective at decreasing bacterial population but are insignificantly different from each other. Error bars correspond to the standard deviations on 6 samples. b) Tukey's multiple comparisons test was performed at 95% confidence intervals. The two groups were significantly different from each other only if the difference between group means ± upper and lower limits did not cross zero (dotted line).

2.4 Discussion

Chitosan polymers with different properties were studied to optimize nanoparticle formulation via ionic gelation. The mechanism behind ionic gelation involves interactions between the positively charged chitosan polymer chains and the negatively charged cross-linking agent TPP under mechanical stirring. MWs and degrees of deacetylation were studied in this work because these factors determine how the chitosan polymer chain interacts with the cross-linker agent TPP (Zhang and Neau 2001; Schiffman and Schauer 2007). The degree of deacetylation determines how many deacetylated sites are available for cross-linking, while MW regulates how accessible these deacetylated sites are.

Based on previously reported work, CNs can be prepared at various concentrations, ranging from 0.1 – 1 mg/mL (Dudhani and Kosaraju 2010; Sullivan et al. 2018), and given a higher concentration formulation is desirable due to greater efficacy, 1 mg/mL for both chitosan and TPP was used for all experiments. Chitosan to TPP mass ratio was studied extensively in an attempt to optimize the formulation. Initially, the average particle diameter of the CNs decreased with increased chitosan to TPP ratio, which can be explained with the increased cross-linking density between chitosan and TPP. However, beyond a certain ratio threshold, CNs started to form aggregates. This could be due to bridging of the nanoparticles by excess chitosan chains. The PDI also followed a similar trend since as chitosan to TPP ratio increased, higher cross-linking density promoted a more uniform size distribution of CNs. However, beyond the critical ratio, the CNs started to aggregate as described above, resulting in higher PDIs. For the zeta potential, a steady increase was observed with increasing chitosan to TPP ratios, since chitosan is positively charged and excess chitosan leads to more cationic nanoparticles. The findings are in agreement with many studies in the literature (Fan et al. 2012; Jonassen et al. 2012). However, the critical ratios differed depending on the MW and degree of deaceytalation of the chitosan polymer.

The optimal formulation was selected based on particle diameter, PDI and zeta potential. The particle diameter is important, because smaller particles have a higher surface to volume ratio, which can therefore adhere to the tooth surface more readily and also swell and contract more easily (Liu et al. 2007). Secondly, PDI is another crucial index

to characterize nanoparticles. It is a dimensionless value generated from a cumulants analysis (2 parameter fit), scaled, and ranges from 0 to 1 for nanoparticles. Values smaller than 0.05 are rare except for highly monodisperse standards. Values greater than 0.7 suggests the size distribution is very broad and means that DLS may not be the best technique to analyze the sample of interest. In general, a lower PDI is better as it indicates a more monodisperse, well-defined sample. Lastly, zeta potential exists between the particle surface and the dispersing liquid. It measures the extent of electrostatic repulsion/attraction between particles and provides insight into the overall stability of nanoparticle suspension and its tendency to aggregate. In general, highly positively/negatively charged nanoparticles form more stable suspensions due to electrostatic repulsions, compared to nanoparticles with zeta potentials close to zero. The optimal formulation will have the best balance of all three parameters. Ideally, it is best to have a formulation with a sub-200 nm nanoparticles in diameter, with a relatively low PDI and a high zeta potential. Through a colloidal stability study by time-course of particle size and PDI measurements by DLS, we found that the nanoparticles maintain their average size and PDI when the zeta potential is above 15 mV. Therefore the ultra-low MW chitosan formulation at a ratio of 6.94:1 (chitosan to TPP) was chosen as it has the smallest particle diameter of 144 $\pm$ 6 nm, with the lowest PDI of 0.15 ± 0.04 at a zeta potential of 18 ± 4 mV. The optimized CNs were visualized by TEM and the average particle diameter estimated from the TEM images was in good agreement with the average particle diameter obtained from DLS. Since HTN3 is a low MW salivary protein, the loading of it into the CNs didn't affect the particle diameter. As shown by the TEM images, there was no general variance in size or dispersity between the unloaded CNs and those with different HTN3 loading ratios.

The pH-responsive properties of the optimized CNs were also investigated. The extent of swelling under different pH conditions was studied. The highest degree of swelling was observed at pH 3 and the CNs remained unchanged at pH 6.3. The results also demonstrated the degree of swelling was proportional to the acidity of the suspension. The swelling response elicited by the pH stimulus was rapid, suggesting that CNs were able to quickly respond to pH changes. The versatility of this pH-responsive property was

further examined through pH cycling between 6.3 and 4, and the results suggested the CNs delivery system was capable of swelling selectively at acidic pH and reversed the swelling process upon removal of the pH stimulus.

The loading loading efficiency of HTN3 was studied at 2%, 5%, and 10% w/w loading ratios of HTN3 to chitosan. The absence of unloaded protein suggested that HTN3 was quantitatively loaded in the delivery system at all ratios, which is beneficial, as the loading can therefore be tuned. Cumulative release studies at different pH values including 3, 4, 5, and 6.8 were also conducted to assess the extent of release of loaded HTN3 from the delivery system. These values were chosen because they reflect the cariogenic conditions promoting different oral diseases. For instance, dental caries initiate at pH 5 and dental erosion occurs at pH 3. In accordance with the demonstration of the pH-responsive property shown previously, the extent of HTN3 release was proportionate to the acidity of the environment. A maximum cumulative release of ~84 ± 7% was achieved at pH 3 over 7 time points, while a minimum release of ~2 ± 2% was observed at pH 6.8. In order to better mimic the pH changes in the oral cavity throughout the day, pH cycling release was performed between pH 6.8 and 4. As presented in the results section, HTN3-loaded CNs were able to selectively release loaded HTN3 at pH 4, and retain the HTN3 at the salivary pH of 6.8. The ability to selectively release HTN3 under acidic conditions is crucial because throughout the day the salivary pH fluctuates many times from the consumption of food or beverages (Bowen 2013). As saliva becomes acidic following carbohydrate intake, the drop in pH could trigger the release of HTN3, which promotes oral homeostasis by inhibiting the demineralization process. Salivary pH would gradually recover to its physiological value due to the buffer capacity of saliva, which would halt HTN3 release from the CNs. Further release of HTN3 would require another incident of sugar ingestion, which would drop salivary pH.

Salivary proteins are known to be susceptible to the high proteolytic activity in the oral cavity, which prevent them from being utilized as potential therapeutics on their own. To evaluate the protection offered by CN against enzymatic degradation, a protein degradation study was performed in 10-fold diluted human saliva. Saliva was diluted to better capture the degradation kinetics of proteins, since at the original concentration the

degradation would have happened too rapidly to allow easy measurement of the process. As presented in the results section, only 6 ± 5 % of the free HTN3 remained at the 2-hour mark. At the same time point, about 47 ± 8 % of HTN3 was still present in the CN delivery system. At the 6-hour mark, only 7 ± 1 % of HTN3 remained in the delivery system, which could be due to the potential breakdown of the CNs by amaylase. Nevertheless, the delivery system prolonged the protein survival time by two-fold. The increase in survival time is important because it allows less frequent administration of the formulation.

Ultimately, a biofilm model was applied to evaluate the therapeutic effect of HTN3-loaded CNs against *S. mutans* biofilm formation on hydroxyapatite discs. *S. mutans* was chosen because it is a major contributor responsible for the initiation and development of tooth decay (Garcia et al. 2017). It metabolizes sucrose to produce sticky polysaccharides which allow the bacteria to aggregate and adhere to the tooth enamel, forming a biofilm. The biofilm, together with frequent sugar intake promotes fermentation of dietary sugar into acidic products. Persistence of the resulting acidic conditions favors the proliferation of acidogenic bacteria. The low pH environment in the biofilm initiates the dental caries process (Argimón and Caufield 2011). Hydroxyapatite is a mineral composed of calcium phosphate, which greatly resembles human hard tissues including bone and tooth enamel in composition and morphology (Wei and Ma 2004). It is also the most stable calcium phosphate mineral under physiological conditions (Kalita et al. 2007). Therefore it has been extensively used in oral applications, such as pellicle formation and biofilm formation (Vacca Smith and Bowen 2000; Takeshita et al. 2015).

Two key factors used to evaluate biofilm growth are biofilm mass and bacterial cell viability. Effective treatment should result in low biofilm mass and reduced bacterial cell viability. For biofilm mass measurements, based on the ANOVA analysis and Tukey's multiple comparisons test, all four treatment groups resulted in significant lighter biofilms than the control group. Fluoride, together with unloaded and HTN3-loaded CNs were significantly more effective than free HTN3. However, no significant difference was observed between the treatment groups. These treatment groups successfully lowered the biofilm mass by at least half. Bacterial cell viability was also determined for all treatment groups. Free HTN3 was not effective at reducing bacterial cell viability and did not perform

better than the control group. Fluoride, unloaded, and HTN3-loaded CNs significantly reduced cell viability when compared against the control group. However, when compared against HTN3, fluoride was not significantly more effective, even though it is significantly more effective than the control group. Unloaded and HTN3-loaded CNs were the most competent treatment groups. They reduced cell viability in half, but their performance in reducing bacterial population were not significantly different from one another. These results suggest that CNs alone can potentially reduce biofilm growth, which could be explained with the functional amino group attacking the cell wall of *S.mutans.* This opens up the possibility of integrating blank CNs directly into dental hygiene products such as mouth wash to prevent dental caries. However, toxicity of these CNs still needs to be determined. Even though HTN3-loaded CNs didn't outperform blank CNs as hypothesized, it is still worth investigating with the optimization of current biofilm model. Future studies can load greater amount of HTN3, or reduce the amount of CNs while maintaining HTN3 concentrations. In addition, CNs are known to exhibit antimicrobial effects against *S.mutans* (Chávez de Paz et al. 2011). Another possible explanation would be CNs alone already prevented the initiation of demineralization, therefore there was no steep drop in pH to trigger HTN3 release from the CNs.

2.5 Conclusion

The results of this study have demonstrated the pH-responsive property of the CNs. The CNs were also able to offer protection against enzymatic degradation in comparison to free HTN3. While HTN3-loaded CNs had successfully reduced biofilm growth as reflected by reduced biofilm mass and bacterial cell viability, it did not significantly outperform unloaded CNs. Future studies should include using the biofilm model to characterize the contribution of HTN3 within CNs and CNs alone in controlling bacterial population. Nonetheless, this work has shown that CNs can be utilized as a protein carrier for oral applications, especially for complications involving acidic environments. This delivery system can also be applied to load other salivary proteins for oral delivery. For instance, HTN1 and HTN5 can be readily loaded into the CNs as they share similar properties as HTN3. Anionic proteins can also be loaded into the CNs with a modified loading protocol. The ultimate goal of this project is to develop a formulation which could be integrated into daily dental hygiene products like toothpaste and mouthwash to provide a preventative approach to address dental caries. Even though blank CNs have demonstrated the potential at reducing biofilm growth, multifunctional salivary proteins-loaded HTN3 is still worth investigating. The results presented in this chapter show that a pH-sensitive delivery system that can release salivary proteins under acidic conditions can be achieved by utilizing a biodegradable, biocompatible, and naturally-derived polymer like chitosan.

2.6 References

Argimón S, Caufield PW. 2011. Distribution of Putative Virulence Genes in Streptococcus mutans Strains Does Not Correlate with Caries Experience. J Clin Microbiol. 49(3):984–992. doi:10.1128/JCM.01993-10.

Basel MT, Shrestha TB, Troyer DL, Bossmann SH. 2011. Protease-Sensitive, Polymer-Caged Liposomes: A Method for Making Highly Targeted Liposomes Using Triggered Release. ACS Nano. 5(3):2162–2175. doi:10.1021/nn103362n.

Basiri T, Johnson ND, Moffa EB, Mulyar Y, Serra Nunes PL, Machado M a. a. M, Siqueira WL. 2017. Duplicated or Hybridized Peptide Functional Domains Promote Oral Homeostasis. J Dent Res. 96(10):1162–1167. doi:10.1177/0022034517708552.

Bowen W. 2013. The Stephan Curve revisited. Odontology. 101(1):2–8. doi:10.1007/s10266-012-0092-z.

Bugnicourt L, Ladavière C. 2016. Interests of chitosan nanoparticles ionically cross-linked with tripolyphosphate for biomedical applications. Prog Polym Sci. 60(Complete):1–17. doi:10.1016/j.progpolymsci.2016.06.002.

Calvo P, Remuñán-López C, Vila-Jato JL, Alonso MJ. 1997. Novel hydrophilic chitosan-polyethylene oxide nanoparticles as protein carriers. J Appl Polym Sci. 63(1):125–132. doi:10.1002/(SICI)1097-4628(19970103)63:1<125::AID-APP13>3.0.CO;2-4.

Carvalho TS, Lussi A. 2014. Combined effect of a fluoride-, stannous- and chitosan-containing toothpaste and stannous-containing rinse on the prevention of initial enamel erosion–abrasion. J Dent. 42(4):450–459. doi:10.1016/j.jdent.2014.01.004.

Cha J, Lee WB, Park CR, Cho YW, Ahn C-H, Kwon IC. 2006. Preparation and characterization of cisplatin-incorporated chitosan hydrogels, microparticles, and nanoparticles. Macromol Res. 14(5):573–578. doi:10.1007/BF03218726.

Chávez de Paz LE, Resin A, Howard KA, Sutherland DS, Wejse PL. 2011. Antimicrobial effect of chitosan nanoparticles on streptococcus mutans biofilms. Appl Environ Microbiol. 77(11):3892–3895. doi:10.1128/AEM.02941-10.

Chen K-J, Chaung E-Y, Wey S-P, Lin K-J, Cheng F, Lin C-C, Liu H-L, Tseng H-W, Liu C-P, Wei M-C, et al. 2014. Hyperthermia-Mediated Local Drug Delivery by a Bubble-Generating Liposomal System for Tumor-Specific Chemotherapy. ACS Nano. 8(5):5105–5115. doi:10.1021/nn501162x.

Costa EM, Silva S, Madureira AR, Cardelle-Cobas A, Tavaria FK, Pintado MM. 2014. A comprehensive study into the impact of a chitosan mouthwash upon oral microorganism's biofilm formation in vitro. Carbohydr Polym. 101:1081–1086. doi:10.1016/j.carbpol.2013.09.041.

Dash M, Chiellini F, Ottenbrite RM, Chiellini E. 2011. Chitosan—A versatile semi-synthetic polymer in biomedical applications. Prog Polym Sci. 36(8):981–1014. doi:10.1016/j.progpolymsci.2011.02.001.

Dudhani AR, Kosaraju SL. 2010. Bioadhesive chitosan nanoparticles: Preparation and characterization. Carbohydr Polym. 81(2):243–251. doi:10.1016/j.carbpol.2010.02.026.

Fábián TK, Hermann P, Beck A, Fejérdy P, Fábián G. 2012. Salivary defense proteins: their network and role in innate and acquired oral immunity. Int J Mol Sci. 13(4):4295–4320. doi:10.3390/ijms13044295.

Fan B, Gillies ER. 2017. Poly(ethyl glyoxylate)-Poly(ethylene oxide) Nanoparticles: Stimuli-Responsive Drug Release via End-to-End Polyglyoxylate Depolymerization. Mol Pharm. 14(8):2548–2559. doi:10.1021/acs.molpharmaceut.7b00030.

Fan W, Yan W, Xu Z, Ni H. 2012. Formation mechanism of monodisperse, low molecular weight chitosan nanoparticles by ionic gelation technique. Colloids Surf B Biointerfaces. 90:21–27. doi:10.1016/j.colsurfb.2011.09.042.

Garcia SS, Blackledge MS, Michalek S, Su L, Ptacek T, Eipers P, Morrow C, Lefkowitz EJ, Melander C, Wu H. 2017. Targeting of Streptococcus mutans Biofilms by a Novel Small Molecule Prevents Dental Caries and Preserves the Oral Microbiome. J Dent Res. 96(7):807–814. doi:10.1177/0022034517698096.

Gusman H, Leone C, Helmerhorst EJ, Nunn M, Flora B, Troxler RF, Oppenheim FG. 2004. Human salivary gland-specific daily variations in histatin concentrations determined by a novel quantitation technique. Arch Oral Biol. 49(1):11–22. doi:10.1016/S0003-9969(03)00182-1.

Helmerhorst EJ, Alagl AS, Siqueira WL, Oppenheim FG. 2006. Oral fluid proteolytic effects on histatin 5 structure and function. Arch Oral Biol. 51(12):1061–1070. doi:10.1016/j.archoralbio.2006.06.005.

Hemadi AS, Huang R, Zhou Y, Zou J. 2017. Salivary proteins and microbiota as biomarkers for early childhood caries risk assessment. Int J Oral Sci. 9(11):e1. doi:10.1038/ijos.2017.35.

Humphrey SP, Williamson RT. 2001. A review of saliva: Normal composition, flow, and function. J Prosthet Dent. 85(2):162–169. doi:10.1067/mpr.2001.113778.

Jonassen H, Kjøniksen A-L, Hiorth M. 2012. Stability of Chitosan Nanoparticles Cross-Linked with Tripolyphosphate. Biomacromolecules. 13(11):3747–3756. doi:10.1021/bm301207a.

Kalita SJ, Bhardwaj A, Bhatt HA. 2007. Nanocrystalline calcium phosphate ceramics in biomedical engineering. Mater Sci Eng C. 27(3):441–449. doi:10.1016/j.msec.2006.05.018.

Kean T, Thanou M. 2010. Biodegradation, biodistribution and toxicity of chitosan. Adv Drug Deliv Rev. 62(1):3–11. doi:10.1016/j.addr.2009.09.004.

Lee ES, Shin HJ, Na K, Bae YH. 2003. Poly(l-histidine)–PEG block copolymer micelles and pH-induced destabilization. J Controlled Release. 90(3):363–374. doi:10.1016/S0168-3659(03)00205-0.

Liu H, Chen B, Mao Z, Gao C. 2007. Chitosan nanoparticles for loading of toothpaste actives and adhesion on tooth analogs. J Appl Polym Sci. 106(6):4248–4256. doi:10.1002/app.27078.

Mandel ID. 1987. The Functions of Saliva. J Dent Res. 66(2_suppl):623–627. doi:10.1177/00220345870660S203.

McDonald EE, Goldberg HA, Tabbara N, Mendes FM, Siqueira WL. 2011. Histatin 1 Resists Proteolytic Degradation when Adsorbed to Hydroxyapatite. J Dent Res. 90(2):268–272. doi:10.1177/0022034510388653.

Mihu MR, Sandkovsky U, Han G, Friedman JM, Nosanchuk JD, Martinez LR. 2010. The use of nitric oxide releasing nanoparticles as a treatment against Acinetobacter baumannii in wound infections. Virulence. 1(2):62–67. doi:10.4161/viru.1.2.10038.

Nikaido T, Moriya K, Hiraishi N, Ikeda M, Kitasako Y, Foxton RM, Tagami J. 2004. Surface analysis of dentinal caries in primary teeth using a pH-imaging microscope. Dent Mater J. 23(4):628–632.

Olivera S, Muralidhara HB, Venkatesh K, Guna VK, Gopalakrishna K, Kumar K. Y. 2016. Potential applications of cellulose and chitosan nanoparticles/composites in wastewater treatment: A review. Carbohydr Polym. 153(Complete):600–618. doi:10.1016/j.carbpol.2016.08.017.

Oppenheim FG, Salih E, Siqueira WL, Zhang W, Helmerhorst EJ. 2007. Salivary proteome and its genetic polymorphisms. Ann N Y Acad Sci. 1098:22–50. doi:10.1196/annals.1384.030.

Puri S, Edgerton M. 2014. How Does It Kill?: Understanding the Candidacidal Mechanism of Salivary Histatin 5. Eukaryot Cell. 13(8):958–964. doi:10.1128/EC.00095-14.

Raafat D, Sahl H. 2009. Chitosan and its antimicrobial potential – a critical literature survey. Microb Biotechnol. 2(2):186–201. doi:10.1111/j.1751-7915.2008.00080.x.

Scarano E, Fiorita A, Picciotti P, Passali G, Calò L, Cabras T, Inzitari R, Fanali C, Messana I, Castagnola M, et al. 2010. Proteomics of saliva: personal experience. Acta Otorhinolaryngol Ital. 30(3):125–130.

Schiffman JD, Schauer CL. 2007. Cross-Linking Chitosan Nanofibers. Biomacromolecules. 8(2):594–601. doi:10.1021/bm060804s.

Shen M, Huang Y, Han L, Qin J, Fang X, Wang J, Yang VC. 2012. Multifunctional drug delivery system for targeting tumor and its acidic microenvironment. J Controlled Release. 161(3):884–892. doi:10.1016/j.jconrel.2012.05.013.

Shimotoyodome A, Kobayashi H, Tokimitsu I, Matsukubo T, Takaesu Y. 2006. Statherin and Histatin 1 Reduce Parotid Saliva-Promoted Streptococcus mutans Strain MT8148 Adhesion to Hydroxyapatite Surfaces. Caries Res Basel. 40(5):403–11.

Siqueira WL, Dawes C. 2011. The salivary proteome: Challenges and perspectives. PROTEOMICS – Clin Appl. 5(11-12):575–579. doi:10.1002/prca.201100046.

Siqueira WL, Lee YH, Xiao Y, Held K, Wong W. 2012. Identification and characterization of histatin 1 salivary complexes by using mass spectrometry. PROTEOMICS. 12(22):3426–3435. doi:10.1002/pmic.201100665.

Siqueira WL, Margolis HC, Helmerhorst EJ, Mendes FM, Oppenheim FG. 2010. Evidence of Intact Histatins in the in vivo Acquired Enamel Pellicle. J Dent Res. 89(6):626–630. doi:10.1177/0022034510363384.

Souza M, Vaz A, Correia M, Cerqueira M, Vicente A, Carneiro-da-Cunha M. 2014. Quercetin-Loaded Lecithin/Chitosan Nanoparticles for Functional Food Applications. Food Bioprocess Technol. 7(4):1149–1159. doi:10.1007/s11947-013-1160-2.

Sullivan DJ, Cruz-Romero M, Collins T, Cummins E, Kerry JP, Morris MA. 2018. Synthesis of monodisperse chitosan nanoparticles. Food Hydrocoll. 83:355–364. doi:10.1016/j.foodhyd.2018.05.010.

Takeshita T, Yasui M, Shibata Y, Furuta M, Saeki Y, Eshima N, Yamashita Y. 2015. Dental plaque development on a hydroxyapatite disk in young adults observed by using a barcoded pyrosequencing approach. Sci Rep. 5:8136. doi:10.1038/srep08136.

Tang WJ, Fernandez JG, Sohn JJ, Amemiya CT. 2015. Chitin Is Endogenously Produced in Vertebrates. Curr Biol. 25(7):897–900. doi:10.1016/j.cub.2015.01.058.

Thandapani G, P. SP, P.n. S, Sukumaran A. 2017. Size optimization and in vitro biocompatibility studies of chitosan nanoparticles. Int J Biol Macromol. 104:1794–1806. doi:10.1016/j.ijbiomac.2017.08.057.

Vacca Smith AM, Bowen WH. 2000. In situ studies of pellicle formation on hydroxyapatite discs. Arch Oral Biol. 45(4):277–291. doi:10.1016/S0003-9969(99)00141-7.

Vitorino R, Calheiros-Lobo MJ, Duarte JA, Domingues PM, Amado FML. 2008. Peptide profile of human acquired enamel pellicle using MALDI tandem MS. J Sep Sci. 31(3):523–537. doi:10.1002/jssc.200700486.

Wei G, Ma PX. 2004. Structure and properties of nano-hydroxyapatite/polymer composite scaffolds for bone tissue engineering. Biomaterials. 25(19):4749–4757. doi:10.1016/j.biomaterials.2003.12.005.

Xiong M, Li Y, Bao Y, Yang X, Hu B, Wang J. 2012. Bacteria-Responsive Multifunctional Nanogel for Targeted Antibiotic Delivery. Adv Mater. 24(46):6175–6180. doi:10.1002/adma.201202847.

Yang X, Grailer JJ, Pilla S, Steeber DA, Gong S. 2010. Tumor-Targeting, pH-Responsive, and Stable Unimolecular Micelles as Drug Nanocarriers for Targeted Cancer Therapy. Bioconjug Chem. 21(3):496–504. doi:10.1021/bc900422j.

Zhang H, Neau SH. 2001. In vitro degradation of chitosan by a commercial enzyme preparation: effect of molecular weight and degree of deacetylation. Biomaterials. 22(12):1653–1658. doi:10.1016/S0142-9612(00)00326-4.

Chapter 3

3 Conclusions and Future Work

3.1 Conclusions

We have developed a reproducible method that yields cationic CNs that successfully loaded HTN3. The HTN3-loaded CNs were able to selectively swell under acidic pH conditions, releasing the loaded HTN3. The amount of HTN3 released was proportional to the acidity of the environment. The observed pH-responsive release is important because the oral cavity acidifies every time after dietary carbohydrate intake. The released protein may promote oral homeostasis to prevent dental caries. Protection of loaded HTN3 against enzymatic degradation was evaluated under the presence of 10-fold diluted human saliva. The delivery system provided a two-fold increase in survival time compared against free HTN3. The prolonged survival time allows the formulation to be administered less frequently, and releases protein to offer protection every time after sugar consumption that happens numerous times a day. Preliminary results have suggested the blank and HTN3-loaded CNs have the potential to reduce biofilm growth, supported by lowered biofilm mass and reduced bacterial cell viability. The most intriguing finding is the blank CNs performed on par with the gold standard fluoride. Results from the biofilm experiment suggested blank CNs alone are sufficient in reducing biofilm growth. One possible application would be to incorporate blank CNs formulation directly into a mouth wash as a preventative measure to address dental caries. Some advantages of using blank CNs alone are the simplified preparation protocol, and reduced cost without HTN3.

There are some limitations to this study. Firstly, the HTN3-loaded CNs were visualized by TEM. However, the 2D-visualization could not explicitly illustrate if HTN3 was loaded inside of the CNs or outside across the surface of CNs. Secondly, the whole saliva was diluted by 10-fold to better capture the degradation kinetics of HTN3, since the degradation would have happened too rapidly at the original concentration, making it a challenge to study. However, this does not simulate the real proteolytic environment. Lastly, the quantity of CNs absorbed onto the HA discs was not quantified due to limitations in methodology.

3.2 Future Work

Future studies can take on two directions. First the possibility of integrating blank CNs into dental hygiene products to prevent dental caries could be further explored. The toxicity profile of the blank CNs needs to be evaluated. Coverage of CNs on tooth surface also needs to be determined.

The second focus would be to continue investigating HTN3-loaded CNs. Saliva collected from caries-active patients will be used to characterize the extent of release from CNs and the kinetics of protein release. Modifications to the preparation of CNs will be attempted to enhance the protection offered against enzymatic degradation. Biofilm experiments will include a larger sample size to compensate for the high sample variability. Treatment time will also be optimized, as only a 2-hour treatment time was evaluated so far. 2 hours is the time required for pellicle formation, but it may not be the optimized time for the attachment of CNs onto the discs. The amount of protein loaded was based on the IC_{50} obtained from the killing assay. More HTN3 can be loaded, and/or lower chitosan concentration should be studied to better distinguish between unloaded and HTN3-loaded CN treatment groups. Another potential treatment group worth investigating would be a combination treatment of HTN3 loaded CNs and fluoride. The newly proposed treatment group is inspired by previous studies in the chemotherapy field that have achieved synergistic effects through combination treatments (Ren et al. 2009; Cai et al. 2015; Mukherjee et al. 2017). A synergistic effect occurs when two or more therapeutic agents combine to create an effect that is greater than the sum of their individual effects. Lastly, the delivery system could also be applied to load other functional salivary proteins, such as HTN1 and HTN5. Other functional salivary proteins could also be loaded through modified loading protocol. A variety of proteins could be loaded to formulate a multifunctional delivery system.

3.3 References

Cai L, Xu G, Shi C, Guo D, Wang X, Luo J. 2015. Telodendrimer nanocarrier for co-delivery of paclitaxel and cisplatin: A synergistic combination nanotherapy for ovarian cancer treatment. Biomaterials. 37(Complete):456–468. doi:10.1016/j. Biomaterials. 2014.10.044.

Mukherjee D, Wu M-L, Teo JWP, Dick T. 2017. Vancomycin and Clarithromycin Show Synergy against Mycobacterium abscessus In Vitro. Antimicrob Agents Chemother. 61(12):e01298-17. doi:10.1128/AAC.01298-17.

Ren H, Tan X, Dong Y, Giese A, Chou TC, Rainov N, Yang B. 2009. Differential Effect of Imatinib and Synergism of Combination Treatment with Chemotherapeutic Agents in Malignant Glioma Cells. Basic Clin Pharmacol Toxicol. 104(3):241–252. doi:10.1111/j.1742-7843.2008.00371.x.

Appendix: Permission to Reuse Copyrighted Material

Title: Stimuli-responsive LbL capsules and nanoshells for drug delivery
Author: Mihaela Delcea,Helmuth Möhwald,André G. Skirtach
Publication: Advanced Drug Delivery Reviews
Publisher: Elsevier
Date: 14 August 2011

Order Completed

Thank you for your order.

This Agreement between Mr. Yi Zhu ("You") and Elsevier ("Elsevier") consists of your license details and the terms and conditions provided by Elsevier and Copyright Clearance Center.

Your confirmation email will contain your order number for future reference.

printable details

License Number	4590270016918
License date	May 15, 2019
Licensed Content Publisher	Elsevier
Licensed Content Publication	Advanced Drug Delivery Reviews
Licensed Content Title	Stimuli-responsive LbL capsules and nanoshells for drug delivery
Licensed Content Author	Mihaela Delcea,Helmuth Möhwald,André G. Skirtach
Licensed Content Date	Aug 14, 2011
Licensed Content Volume	63
Licensed Content Issue	9
Licensed Content Pages	18
Type of Use	reuse in a thesis/dissertation
Portion	figures/tables/illustrations
Number of figures/tables/illustrations	1
Format	both print and electronic
Are you the author of this Elsevier article?	No
Will you be translating?	No
Original figure numbers	Figure 1
Title of your thesis/dissertation	a pH-sensitive Delivery System for the Prevention of Dental Caries Using Salivary Proteins
Expected completion date	Jun 2019
Estimated size (number of pages)	85

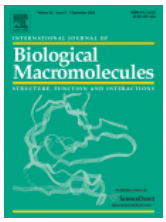

Title: A review on chitosan and its nanocomposites in drug delivery

Author: Akbar Ali,Shakeel Ahmed

Publication: International Journal of Biological Macromolecules

Publisher: Elsevier

Date: 1 April 2018

Order Completed

Thank you for your order.

This Agreement between Mr. Yi Zhu ("You") and Elsevier ("Elsevier") consists of your license details and the terms and conditions provided by Elsevier and Copyright Clearance Center.

Your confirmation email will contain your order number for future reference.

printable details

License Number	4590270392555
License date	May 15, 2019
Licensed Content Publisher	Elsevier
Licensed Content Publication	International Journal of Biological Macromolecules
Licensed Content Title	A review on chitosan and its nanocomposites in drug delivery
Licensed Content Author	Akbar Ali,Shakeel Ahmed
Licensed Content Date	Apr 1, 2018
Licensed Content Volume	109
Licensed Content Issue	n/a
Licensed Content Pages	14
Type of Use	reuse in a thesis/dissertation
Portion	figures/tables/illustrations
Number of figures/tables/illustrations	1
Format	both print and electronic
Are you the author of this Elsevier article?	No
Will you be translating?	No
Original figure numbers	Figure 1
Title of your thesis/dissertation	a pH-sensitive Delivery System for the Prevention of Dental Caries Using Salivary Proteins
Expected completion date	Jun 2019
Estimated size (number of pages)	85

Curriculum Vitae

Name: Yi Zhu

Post-secondary Education and Degrees:

Western University
London, Ontario, Canada
2017-2019 M. ESc.

University of Toronto
Toronto, Ontario, Canada
2012-2016 B. Sc.

Related Work Experience

Teaching Assistant
Western University
2017-2019

Presentations:

Zhu, Y; Siqueira, W. L.; Gillies, E. R. "A pH-sensitive Delivery System for the Prevention of Dental Caries Using Salivary Protein." Fallona Family Research Showcase, London, Canada, April 12, 2018, poster.

Zhu, Y; Siqueira, W. L.; Gillies, E. R. "pH-sensitive Chitosan Nanoparticles: A Novel Approach to the Prevention of Dental Caries." 34th Annual Meeting of the Canadian Biomaterials Society, Victoria, Canada, May 16-19, 2018, poster. (awarded CBS Travel Award worth of $600)

Zhu, Y; Siqueira, W. L.; Gillies, E. R. "A pH-sensitive Delivery System for the Prevention of Dental Caries Using Salivary Protein." School of Biomedical Engineering Seminar, London, Canada, November 13, 2018, Oral.

Zhu, Y; Siqueira, W. L.; Gillies, E. R. "Prevention of Tooth Decay." 3 Minute Thesis, London, Canada, January 21, 2019, oral.

Zhu, Y; Siqueira, W. L.; Gillies, E. R. "A pH-sensitive Delivery System for the Prevention of Dental Caries Using Salivary Protein." Western Research Forum, London, Canada, March 22nd, 2019, poster.

Zhu, Y; Siqueira, W. L.; Gillies, E. R. "A pH-sensitive Delivery System for the Prevention of Dental Caries Using Salivary Protein." Centre for Advanced Materials and Biomaterials Research (CAMBR) Research Day, London, Canada, April 17th, 2019, both oral and poster.